

Toponium

I. M. Dremin

P. N. Lebedev Physics Institute, Academy of Sciences of the USSR, Moscow
Usp. Fiz. Nauk **150**, 185–219 (October 1986)

The bound system of top and antitop quarks, called toponium, can be used for spectroscopic studies at distance scales of less than 10^{-14} cm. Physics at such short distance scales is an abundant source of new information. The possibilities of creation of new particles in toponium decays, the determination of quark structure from spectroscopic data on toponium, and the verification of basic ideas on strong and electroweak interactions are reviewed.

CONTENTS

1. Introduction.....	903
2. Charmonium and bottomium.....	904
3. General properties of potential models.....	905
4. New range of distances.....	907
5. Toponium spectroscopy.....	909
6. Toponium decay modes.....	911
6.1. General information. 6.2. Scalar Higgs particles. 6.3. Supersymmetric particles.	
6.4. The structure of quarks and Λ_{QCD} . 6.5. Number of types of neutrino. 6.6. The	
Weinberg angle. 6.7. Interference of toponium and the Z^0 -bosons.	
7. Production of toponium.....	918
8. Conclusions.....	920
Appendix.....	921
References.....	922

1. INTRODUCTION

The discovery of the J/ψ particle in 1974 was the starting point for a detailed spectroscopic study of the properties of the quark-quark interaction at small separations. This particle consists of the relatively heavy charmed quark c and its antiquark \bar{c} , and is the progenitor of a whole family of bound states with hidden charm, i.e., the charmonium family.

The analogous family of particles consisting of the still heavier bottom quark b and its antiquark \bar{b} , the bottomium family, was discovered four years later.

The greater bound-state mass signifies a transition to more compact systems, i.e., it offers the possibility of studying quark interactions at still shorter distances. Theory predicts the existence of the top quark t , which is expected to be much heavier than the bottom quark. While the masses of the charmed and bottom quarks are equal to about 1.5 and 5 GeV, respectively, the mass of the top quark is definitely greater than 23 GeV (judging by the results of experiments on the PETRA accelerator¹), and is probably in the range between 30 and 50 GeV (as indicated by preliminary data obtained by the Uda1 collaboration on the Sp \bar{p} S collider²). It is therefore hoped that it will soon be possible to detect a new family of particles with a hidden top, namely, the toponium family,¹⁾ using the soon to be commissioned electron-positron SLC accelerator (beginning of 1987) and the LEP accelerator (end of 1988). These machines will initially produce energies of 50×50 GeV and, later, 100×100 GeV (on LEP II). Of course, the first task will be to investigate the properties of the Z^0 boson. However, studies of toponium

will not only extend existing results, but may well produce much new material.

These new machines will provide us with a first opportunity for accurate spectroscopic measurements at distance scales of less than 10^{-14} cm. Bound states of systems as small as this have not been encountered in physics before, and interest in such objects arises from the fact that strong, electromagnetic, and weak processes begin to rival one another on an equal footing at short distances. Naturally, by entering a new range of distances, it may be possible to discover fundamentally new phenomena.

What is it that studies of the toponium family are theoretically expected to produce?

First, the greatest interest would be attracted by the discovery of the neutral scalar Higgs particle—the last (and very important) element of the standard model of electroweak interactions that has not yet been seen.

It will be shown below that this will become possible by studying toponium decays if the mass of the Higgs particle does not exceed 80–90% of the mass of toponium. The precision with which its mass will be determined in this way may even be better than 1 GeV.

As far as charged Higgs particles are concerned, their detection, if they exist at all, will be a very simple matter in this mass range.

Second, the discovery of supersymmetric partners of ordinary particles among the toponium decay products would inject new life into supersymmetry theory.

Third, toponium spectroscopy would be capable of yielding information on the transition from current to con-

stituent quarks, and on the role of the dynamic mass of the quark at short distances. In particular, this would help in solving the problem of chiral symmetry in the case of light quarks. It would actually be the beginning of the spectroscopic study of the internal QCD structure of the quark.

Fourth, the decay of toponium into a neutrino and antineutrino may well provide a new method for counting the number of neutrino species, which may lead to the physics of new generations. However, this will probably be done at an even earlier stage by measuring the width of the Z^0 resonance so that, in this respect, toponium will merely confirm the results of such experiments.

It may be that other lines of research bearing on the study of toponium but which to some extent have already been involved in the analysis of other processes or have been fairly reliably predicted by theory will not be as new or as fundamental for the development of theory, but will still be quite important. They may be summarized as follows.

1. Measurements of the relative fraction of different decay modes of the top quark can be used to estimate its lifetime and to determine the Kobayashi-Maskawa matrix element V_{th} , which is responsible for the transformation of the top quark into the bottom quark (and, possibly, also the off-diagonal elements V_{ts} and V_{td}).

2. The spectroscopy and decay modes of low-lying energy levels of the toponium family will resolve (directly, for the first time) the problem of the asymptotic freedom parameters (spectroscopic data will be used to determine the chromodynamic parameter Λ_{QCD}).

3. The spectroscopy of high-lying toponium levels is important for the additional verification of the flavor independence of the quark-quark potential.

4. Measurement of angular asymmetries in the decay of toponium (and also away from resonance) into a lepton pair, analysis of leptons from semileptonic decays of the top quark, studies of polarization asymmetries in the interaction between longitudinally polarized beams, and studies of the azimuthal symmetry in the interaction of transversely polarized beams should enable us to determine the strength of coupling between the neutral current and the top quark, i.e., to determine independently the Weinberg angle (it has been suggested that the precision with which $\sin^2\theta_w$ will be determined will be of the order of 4×10^{-3}). Moreover, these measurements will verify once again the charge of the top quark and its isospin.

The physics of toponium is thus seen to hold much promise, and this makes it a very attractive object for investigation. It is, however, important to emphasize also the further fact that, although the theory is not capable of predicting the mass of toponium, it is very ready for the interpretation of spectroscopic data on toponium and of its decay modes as soon as the toponium mass becomes available.

The aim of this review is specifically to provide a brief but reasonably complete description of the different theoretical predictions for the toponium family, to discuss the physical consequences of these predictions, and, hence, to prepare the reader for the arrival of the extensive experimental material on toponium that will, undoubtedly, soon ap-

pear on the pages of physics journals. The bound states of heavy quarks, i.e., the quarkonia, have been under discussion for some considerable time, and the review literature in this field, which to some extent is relevant for toponium, is very extensive (see, for example, Refs. 3–23). We shall not be able, within the confines of a single review, to describe all the details of theoretical approaches and estimates, or to reproduce the numerous tables and graphs that predict particular toponium parameters in different potential models. Readers wishing to become familiar with such details must turn to the original or review papers, to which references are given in text.

We shall start by recalling the properties of the lighter charmonium and bottomium families (Sec. 2) and, having enumerated the lessons drawn from studies of potential models (Sec. 3), we shall proceed to attempts to extrapolate them to shorter distances (Sec. 4). This will be followed by a discussion of physical consequences and different possibilities for the spectroscopy of toponium (Sec. 5) and its decay modes (Sec. 6). The question of the production and detection of toponium will be briefly discussed only at the end (Sec. 7). The basic conclusions of the present review will be summarized in the last section (Sec. 8). The question of the QCD radiative corrections to the theoretical calculations of the different toponium parameters will be examined in the Appendix.

2. CHARMONIUM AND BOTTOMIUM

The properties of the charmonium and bottomium families have now been relatively well (although not completely) investigated and described in many review papers (we recall Refs. 3–23, and note the further Refs. 24–31). We shall therefore confine ourselves to a brief recapitulation, emphasizing typical general features that will be important for our subsequent discussion of the basic properties of toponium.

Heavy-quark systems have attracted attention because their parameters can be used to investigate both the static properties of quarks and the dynamics of their interaction. Such studies are facilitated (in particular, as compared with light quarks) by a number of factors. First, these are the simplest two-particle systems consisting of a quark and an antiquark. Second, they are true bound states (and not merely quasibound states, such as those formed by ordinary mesons, e.g., the ρ meson, and so on). Third, the velocities of quarks in quarkonia are nonrelativistic, so that nonrelativistic quantum mechanics can be employed. Fourth, the small size of quarkonia enables us to examine one of the basic assumptions of quantum chromodynamics, i.e., the property of asymptotic freedom.

Spectroscopic studies of charmonium and bottomium are very similar: they include measurements of level energies, the total, hadronic, and leptonic level widths, and the hadronic and radiative transitions between the levels.

This abundance of experimental information enables us to learn the behavior of the wave function of the system over a wide range of distances. The data can also be used to extract information on the shape of the interaction potential

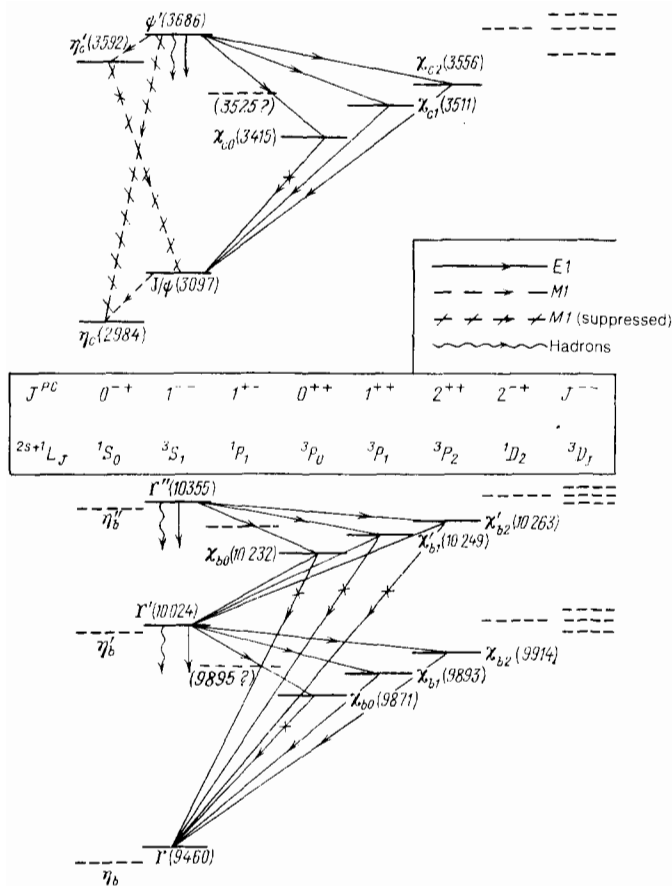


FIG. 1. Energy level scheme and radiative and hadronic transitions in charmonium (a) and bottomium (b) below the threshold for the creation of particles with bare flavor.

and its dependence on the quark flavor, the spin-orbit and spin-spin interactions between quarks, their electric and color charges, the nonpotential and relativistic effects, the role of channels of decay into particles with bare flavor, and so on.

Figure 1 shows the energy-level schemes of charmonium and bottomium below the threshold for the production of a particle with bare flavor. The spectroscopic level symbols ($^{2s+1}L_J$ and J^{PC}) are indicated together with the symbols (J/ψ , ψ' , χ , χ' , and so on) for the ground state and its radial excitations, the masses of the corresponding particles²⁾ (in MeV), and the radiative and hadronic transitions between the energy levels. A solid line is used to indicate experimentally confirmed levels, while broken lines show levels that have been predicted by potential models, but have not yet been seen experimentally. Transitions between known levels that have not been recorded, or adequately studied experimentally, are indicated by a cross.

We recall that the splitting of the χ -level triplets is due to the spin-orbit interaction, and the shift of the η -levels relative to the 3S_1 states, which are directly created in e^+e^- collisions, is due to the spin-spin interaction, i.e., both effects are a consequence of relativistic corrections that are not directly taken into account in the Schrödinger equation. In quarkonium spectroscopy, the ground state and its radial excitations (for given orbital angular momentum L) are

usually labeled by the number $n_r + 1$ (n_r is the radial quantum number indicating the number of zeros of the wave function), which appears in front of the spectroscopic symbol $^{2s+1}L_J$. This distinguishes the notation from the notation used in atomic spectroscopy in which the principal quantum number $n = n_r + L + 1$ is employed.

$$n = n_r + L + 1.$$

The most interesting feature of the spectroscopy of quarkonia is clearly seen in Fig. 1. It is the relative disposition of the χ_c levels (1^3P_J) and the ψ' level (2^3S_1), and, correspondingly, χ_b (1^3P_J) and Υ' (2^3S_1), and also χ'_b (2^3P_J) and Υ'' (3^3S_1). The 2S and 1P ($3S$ and $2P$, etc.) levels are degenerate in the case of Coulomb interaction (for example, in the hydrogen atom).³⁾ In quarkonia, the 1P level lies below the 2S, and the 2P level below the 3S.

It is also interesting to note that the level separation between the 2^3S_1 and 1^3S_1 states is almost the same in both families (it is a little greater in the case of charmonium).

We also note the characteristic splitting of the P-level triplet, whereby the state with lower total angular momentum lies below the state with higher angular momentum. Extensive information is available also on the decay widths of charmonium and bottomium and on transitions between the different states shown in Fig. 1. We shall not reproduce it here and refer the reader to review papers.³⁻³¹ We merely note an important general feature, namely, that all the widths are several times greater in charmonium than in bottomium.

All these characteristic features of the spectroscopy of charmonium and bottomium can be quantitatively reproduced with sufficient accuracy (see, for example, Ref. 17) by potential models, using the Schrödinger equation or its simplest relativistic generalizations (the Breit-Fermi equation, etc.). The potential approach is particularly successful, and widely used, in the description of the properties of particles that have already been discovered and in the prediction of new members of these families (for example, the prediction of the position of the center of the triplet of χ_b states³² and the leptonic width of bottomium^{33,34}). Of course, and this must be emphasized, the entire approach is phenomenological and necessitates the determination of model parameters by comparison with experimental data, but this is compensated, at least to some extent, by the range of the available experimental information. Closer to the fundamentals of the theory is the QCD sum rule, which has successfully predicted the η_c , but has not been successful with the χ_b . Moreover, this approach is valid only for low-lying states, and is practically ineffective in the region of toponium (although it is used to verify the validity of potential models; see footnote 8). For us, the only significant qualitative results will be those ensuing from potential models that can be used to examine the consequences of a particular extrapolation into the toponium region. We now turn to these results.

3. GENERAL PROPERTIES OF POTENTIAL MODELS

A nonrelativistic two-body system, held together by spherically symmetric forces, is described by the Schrödinger equation⁴⁾

$$-\frac{1}{2\mu} \Delta \Psi(\mathbf{r}) + [V(\mathbf{r}) - E] \Psi(\mathbf{r}) = 0, \quad (1)$$

where $\mu = m_1 m_2 / (m_1 + m_2)$ is the reduced mass of the system consisting of quarks of mass m_1 and m_2 , \mathbf{r} is the separation between them, $V(\mathbf{r})$ is the interaction potential, E is the energy of the system, and $\Psi(\mathbf{r})$ is its wave function. In the case of a spherically symmetric potential $V(r)$, Eq. (1) assumes the form

$$u'' + 2\mu \left[E - V(r) - \frac{l(l+1)}{2\mu r^2} \right] u(r) = 0, \quad (2)$$

$$u(0) = 0, \quad u'(0) = R(0), \quad \Psi(r) = R(r) Y_{lm}(\theta, \varphi),$$

$$u(r) = rR(r);$$

where $R(r)$ is the radial wave function and l the orbital angular momentum quantum number.

To solve (2), we must know the form of the potential $V(r)$ and the reduced mass μ . Since quarks have not been observed in free states, their masses are not adequately known, and the quantity μ is usually looked upon as an adjustable parameter, to be determined from the spectrum of the corresponding quarkonium family.

Still greater (functional) arbitrariness arises in the choice of the interaction potential $V(r)$ between the quark and the antiquark in quarkonium. Since numerous experimental data have to be described, this naturally selects the shape of the potential virtually unambiguously in a certain restricted range of distances under investigation, so that one would hope that this approach will yield important information on the nature of the interaction between quarks in this range.

The simplest qualitative information on the interaction between quarks in quarkonia can be obtained from the properties of the lowest-lying levels of this system, without describing, for the moment, the entire range of experimental data. Many general relationships follow (even if we do not know the specific interaction potential) from the theorem on the Wronskian (e.g., the number of nodes in the wave function). They are described in textbooks on quantum mechanics.

A new and very interesting result^{32,36} is concerned with the order in which the energy levels of bound states appear. It has been shown that, in the case of a non-Coulomb potential, levels with the same principal quantum number lie lower for the same high values of l if the potential is concave relative to the Coulomb potential, i.e., if the following condition is satisfied throughout:

$$\Delta_r V(r) \equiv \frac{1}{r^2} \frac{d}{dr} \left(r^2 \frac{dV}{dr} \right) > 0. \quad (3)$$

Correspondingly, the reverse situation, $E(n, l) < E(n, l+1)$, occurs if the convexity condition $\Delta_r V < 0$ is satisfied and the potential increases monotonically ($dV/dr > 0$) for all r .

Moreover, it can be shown that $E(n, l) \leq E(n-1, l+2)$ if the following conditions are satisfied throughout:

$$\frac{d}{dr} \left(\frac{1}{r} \frac{dV}{dr} \right) \geq 0, \quad (4)$$

and also $E(n, l) < E(n-1, l+3)$ for

$$r \frac{d^2 V}{dr^2} \leq 3 \frac{dV}{dr}. \quad (5)$$

The simplest example of the application of (3) is as follows: having found that the 1P level lies below the 2S level in quarkonia, we may conclude that we are not entitled to use monotonically increasing potentials for which the Laplacian is negative throughout. Additional restrictions on the shape of the potential can be deduced from the relative disposition of the 1D and 2S levels [condition (4)], or the 1F and 2S levels [condition (5)].

The overall qualitative behavior of low-lying states of the quark-antiquark system as functions of mass (or effective distance) can be deduced from general theoretical principles such as the virial theorem and the uncertainty relation (see, for example, Refs. 7, 13, 20, and 21).

It is well-known that the virial theorem relates the mean kinetic energy T of a system and the potential as follows:

$$\langle T \rangle = \frac{1}{2} \left\langle r \frac{dV}{dr} \right\rangle, \quad (6)$$

whereas the uncertainty relation gives

$$\langle p^2 \rangle \langle r^2 \rangle \geq 1. \quad (7)$$

If, in subsequent qualitative estimates, we neglect the spread in the corresponding variables and, omitting the averaging symbols throughout, take R and M to represent the effective size and mass of the systems, then, using (6) and (7), we can readily obtain general qualitative relationships for many physical parameters as functions of the radius of the system and of the average rate of increase in potential, dV/dR . For example, substituting $T \sim mv^2/2$ and $p \sim mv$ in (6) and (7), we find that the average velocity v of quarks in quarkonium depends on the size of the system and the shape of the potential as follows:

$$v \sim R^2 \frac{dV}{dR}. \quad (8)$$

Hence, it follows that, for potentials with a positive Laplacian, the average quark velocity increases with increasing size of the system. The mass and size of the system are related by

$$m \sim \left(R^3 \frac{dV}{dR} \right)^{-1}. \quad (9)$$

We can now use the Schrödinger equation (2) to obtain^{7,21} the general relation for S-wave functions:

$$|R(0)|^2 \sim m \frac{dV}{dR} \sim R^{-3} \quad (10)$$

which turns out to be important for the understanding of the qualitative behavior of the leptonic width Γ_l of quarkonium S-levels, since it shows [if we use (9), (10), and (27) for these levels] that it is very sensitive to the derivative of the potential:

$$\Gamma \sim |R(0)|^2 m^{-2} \sim R^3 \left(\frac{dV}{dR} \right). \quad (11)$$

To make these relationships and the conclusions that ensue from them physically clearer, it is useful to approximate the potential by a power-type function of distance:

$$V(r) = \alpha r^k, \quad (12)$$

where it is assumed that this approximation is always possible in some restricted range of effective distance. It is then an easy matter to rewrite (8)–(11) so as to emphasize the dependence of the different variables on the physically interesting parameter m , i.e., the mass of the system consisting of heavy quarks.^{7,21} However, these relationships are still not very interesting in this very general form. They may be of practical value (in the context of the physics of quarkonium) in two special cases, namely, small $\varepsilon \ll 1$ and the near-Coulomb case $\varepsilon \simeq -1$. The former corresponds to the phenomenological potential^{7,37} that is a slowly-varying function of r and provides a good description of experimental data on charmonium and bottomium, whereas the latter is close to the asymptotically free interaction between quarks, which we hope to discover in toponium.⁶⁾ Thus, comparison of these two possibilities will help us to detect tendencies in the variation of particular variables as we pass to heavier system. The following is a list of the corresponding results for the Coulomb case $\varepsilon = -1$ (indicated by the letter C) and the case $2\varepsilon \ll 1$, neglecting 2ε in comparison with unity (this is denoted by CB, which stands for “charmonium, bottomium”):

$$R \sim m^{-1} (C), \quad m^{-1/2} (CB), \quad (13)$$

$$v \sim m^0 (C), \quad m^{-1/2} (CB), \quad (14)$$

$$|R(0)|^2 \sim m^3 (C), \quad m^{3/2} (CB), \quad (15)$$

$$\Gamma_c \sim m (C), \quad m^{-1/2} (CB), \quad (16)$$

$$\Delta E \sim m (C), \quad m^{-\varepsilon/2} (CB), \quad (17)$$

$$\Gamma(E1) \sim m (C), \quad m^{-1} (CB), \quad (18)$$

$$\Delta E_{ss} \sim m(C), \quad m^{-1/2} (CB). \quad (19)$$

Apart from the general formulas given earlier for the four variables, we have also used in these expressions the corresponding formulas and estimates for the radial splitting ΔE of low-lying levels, the radiative width $\Gamma(E1)$ of E1 transitions, and the spin-spin splitting ΔE_{ss} [for a δ -function potential describing the spin-spin interaction; see also (26)].

If we scan the second column, we can readily see the above basic regularities as we pass from charmonium to bottomium: the size of the system decreases, the nonrelativistic condition $v \ll 1$ is more easily satisfied, the leptonic and radiative widths decrease, the 2S–1S splitting is practically constant, and, finally, we have the predicted reduction in the $\Upsilon - n_b$ splitting as compared with $J/\psi - \eta_c$.

If we look horizontally from left to right, we are led to a qualitative understanding of what we might legitimately expect in toponium: a reduction in the size of the system for a slight improvement in the nonrelativistic condition (but we note that quarks are sufficiently nonrelativistic even in the case of bottomium), and an increase in the level width and level splitting as compared with bottomium.

In these estimates, we have actually discarded the possibility (which is, in fact, not very likely in the light of QCD and asymptotic freedom) of a continuous extrapolation of the quasilogarithmic potentials^{7,37} with $\varepsilon \ll 1$ into the toponium region, and have assumed that this phenomenological dependence, which has been observed in charmonium and bottomium, will pass continuously into an asymptotically free dependence. Although the above forms of asymptotical-

ly free potentials with monotonic interpolation to confinement are quite different (see the review in Ref. 17), and lead to somewhat different predictions for toponium, it is very easy to be diverted into a physically unprofitable examination of small differences between them. We hope that nature is not so monotonic and depressing, and may reveal new effects in this distance range.

4. NEW RANGE OF DISTANCES

Continuing with our theme of potential models, we must emphasize that, even in the case of charmonium and bottomium, the choice of a particular potential is dictated either by the desire to describe experiments by the simplest formula (as in the case of the quasilogarithmic potentials), or by attempts to interpolate the asymptotically free potential at short distances and the linearly increasing confining potential at large distances. The interpolation is performed so that, in the intermediate range of distances typical for charmonium and bottomium (between approximately 0.3 and 1 fm), the two potentials are numerically practically indistinguishable. This is why a satisfactory description of experiments is achieved in both cases, although there are appreciable discrepancies between theory and experiment in the case of hadronic widths, which are ascribed to large radiative corrections that have not been taken into account (see Appendix), and there is some concern about the large value of the constant Λ_{QCD} (about 400 MeV) deduced from the requirement that such interpolations must agree with experiment.

According to experimental data on deep inelastic processes, for distances in the range typical for toponium (from 0.05 fm), asymptotic freedom should already be fully manifest, and the interaction potential should correspond to single-gluon exchange with $\Lambda_{\text{QCD}} = \Lambda_{\text{MS}} \simeq 100$ MeV:

$$V(r) \xrightarrow{(r \rightarrow 0)} -\frac{4}{3r} \cdot \frac{12\pi}{(33 - 2n_f) \ln(1/r^2 \Lambda_c^2)}, \quad (20)$$

where $\Lambda_c = e^C \Lambda_{\text{MS}}$ and $C = 0.5772 \dots$ is the Euler constant.

A possible way out of the resulting situation may be indicated by the fact that a transition from current to constituent quarks occurs at these distances. Actually, (20) is valid only for current quarks, whereas for transferred momenta $q^2 \sim 1 \text{ GeV}^2$, i.e., for distances ~ 0.1 fm, current quarks should be dressed by the gluon field and become constituent quarks. The mechanism responsible for this transition is still not clear, but there are indications that the transition is quite abrupt.^{38,39} It is known from experiment that both u, d, and the heavier s quark acquire an additional mass of about 300 MeV in this transition. If the dynamics of this process does not depend on the quark flavor, this will also occur in the case of c, b, and t quarks and, hence, the relatively small toponium should sense the change in the quark mass.

How can this transition affect toponium? Not surprisingly, the answer to this question is related to the problem of quark confinement, i.e., it originates in the region of large distances. It has long been known⁴⁰ that the solution of the Dirac equation with a centrally symmetric field that in-

creases linearly with distance does not produce bound states.⁷⁾ Bound states are obtained only by introducing the Lorentz-scalar confining potential,⁴¹ widely used to describe quarkonia (see, for example, Refs. 42–51 and the references therein), especially to explain the disposition of the 3P_J levels and the splitting of the ortho- and para-levels ($\Upsilon - \eta_b$, etc.), i.e., in spin-orbit and spin-spin interactions. The Lorentz-scalar part appears in the usual potential in the Schrödinger equation additively with the Lorentz-vector component, and cannot therefore be separated in a completely nonrelativistic description. However, it influences the above relativistic effects because it appears in them in a nonadditive manner.

The physical meaning of the Lorentz-scalar potential is very clear:⁵² If we treat quarks as objects whose mass depends on relative distance, we find that it is precisely this mass that plays the part of the Lorentz-scalar potential. It is common to draw attention only to the fact that this dependence becomes manifest at large distances and assures quark confinement. The commonly accepted treatment of the structure of the quarkonium potential is therefore as follows: the Lorentz-vector part of the potential (single-gluon exchange with asymptotic freedom) is the predominant effect at short distances, the Lorentz-scalar confining part predominates at large distances, and smooth interpolation with a varying proportion of the two components can be used in the intermediate region. We have already noted that one consequence of this treatment is that it is difficult to reproduce the asymptotically free contribution with the correct value of Λ_{QCD} .

However, the variation in the mass of the quark at short distances that accompanies the transition from current to constituent quarks should also manifest itself as a variation in the Lorentz-scalar potential. If this variation occurs rapidly, i.e., within a very small range of distances, the smoothness of the interpolation is destroyed, and the potential should contain a “jump”^{53,54} by about 600 MeV (in the case of two quarks, each should acquire a mass of 300 MeV), which should occur at distances of about 0.1 fm.

Since the potential is then shallower at short distances (because of the lower value of Λ_{QCD}), the average derivative of the potential over a large enough interval will remain the same and, according to (8), (9), and (11), the basic consequences for charmonium and bottomium (quark velocity, average size, leptonic width, and so on) will be unaffected, except for the hadronic widths, which are proportional to α_s^3 for the 3S_1 levels. They become appreciably closer to the experimental values because of the larger value^{53,54} of Λ_{QCD} .

The properties of toponium become significantly different (see later Sections) as compared with the prediction for quasilogarithmic potentials and for continuous interpolations between asymptotic freedom and confinement.

Figure 2 illustrates the above three types of potential. We emphasize that the potential with a “step” differs noticeably from the other two potentials by the fact that it does not satisfy condition (3) [which is valid for potentials (12) with $\kappa > 0$, $\varepsilon > 0$ and (20)]. The Laplacian of the potential has a variable sign in this case.

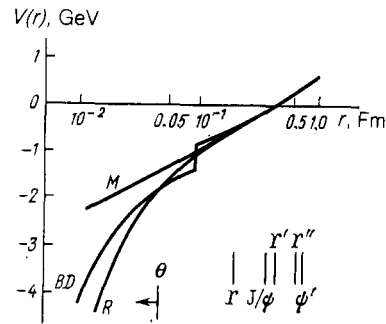


FIG. 2. Interaction potentials in quarkonia: M —quasilogarithmic,³⁷ R —asymptotically free with monotonic interpolation to linear confinement,³² BD —asymptotically free with a step (due to the transition between current and constituent quarks) during interpolation to linear confinement.⁵³

The important point here is that the QCD perturbation theory is valid (with the correct magnitude of Λ_{QCD}) only until we reach distances of the order of 0.1 fm, for which we have to deal with current quarks, and the subsequent region, i.e., the interaction of constituent quarks, is treated purely phenomenologically until it becomes possible to calculate correctly the nonperturbative effects in QCD. It is significant that the two regions are now very clearly separated.⁸¹⁾

Thus, toponium may turn out to be very sensitive to the nature of the transition between current and constituent quarks, and may help us to reveal the QCD structure of quarks.

Of course, for us, it is more interesting to verify the predictions of the *theory* (in the present case, QCD) than to examine the consequences of *models*. Nevertheless, an experimental confirmation of the model with a “step” would lead to important consequences for QCD calculations of the kind performed in Refs. 55 and 56 by demonstrating the appreciable role of nonperturbative effects at distances as small as 0.1 fm.

As already noted, the novelty of the physics of toponium is that we shall be dealing for the first time with a system for which the effects of electroweak interactions become comparable with those of strong interactions. This will be clearly demonstrated when we consider the toponium decay modes in Sec. 6. Thus, as we deduce the consequences for QCD, we will also be able to obtain new data on the electroweak processes. Of course, searches for the neutral Higgs boson must be given priority. Unfortunately, the theory does not predict its mass. It will be shown below that this particle will be noticeable among the toponium decay products if its mass is somewhat lower than the mass of toponium.

It is well-known⁵⁷ that electrically charged Higgs bosons appear in models of the electroweak interaction that are more complex than the standard model. It will be a very simple matter to detect such particles (given that they exist) in toponium decays (for the corresponding masses).

Because the distances are so short, pure neutrino decays play a more important part, and may yield information on the number of types of neutrino.

Determinations of the Kobayashi-Maskawa matrix ele-

ment V_{tb} and accurate measurements of the Weinberg angle complement the possibilities of toponium in the elucidation of the physics of electroweak processes.

Finally, the discovery of the supersymmetric partners of particles among the toponium decay products would, of course, be a major sensation. Once again, the weak point of the theory is that it is not able to predict the masses of these particles.

Summarizing, we are led to the conclusion that physics at short distances may turn out to be more fertile than we have suggested. However, even the possibilities of toponium physics that were examined above are of great importance for our understanding of both strong and electroweak interactions and of the symmetry properties of the particle world.

5. TOPONIUM SPECTROSCOPY

The number of toponium levels⁹⁾ above the threshold for the creation of bare top particles turns out to be appreciably greater than in either charmonium or bottomium. Of course, to predict this number correctly, we must know the detailed behavior of the interaction potential. However, the situation becomes much simpler because, first, this number is determined by the enormous number of practically overlapping levels with high orbital angular momenta, i.e., the quasiclassical approach can be used in approximate calculations, and, second, all the proposed potentials are steeper than the Coulomb potential at large distances, because of the confining components, and this provides us with a lower bound for the total number of levels. Quasiclassical estimates⁵⁸ made on the assumption that the binding energy of the light quark in the system containing a heavy quark is independent of the mass of the latter⁵⁹ show that the number of S-states of toponium created directly in e^+e^- annihilation is approximately given by

$$n_S \approx 2 \left(\frac{m_t}{m_c} \right)^{1/2}, \quad (21)$$

where m_t and m_c are the masses of the top and charmed quarks. The total number of levels must exceed (for given n_S) the number in the Coulomb potential, i.e.,

$$n_T \geq 2n_S + 4 \sum_{l=1}^{n_S-1} (n_S - l) - 2n_S^2, \quad (22)$$

where we have taken into account the hyperfine splitting of the S levels (the factor 2 in the first term) and the presence of four levels (the $J = L$ level and the three levels corresponding to fine structure) for $L > 0$.

It follows from these formulas that, when the mass of the top quark is approximately 40 GeV, there should be about 10 particles with mass below the threshold for the creation of the bare top (i.e., narrow states) directly in e^+e^- collisions, and the entire toponium family should have in excess of 200 narrow states. Calculations²⁰ performed for a specific potential (indicated by the letter R in Fig. 2),³² assuming that the mass of the top quark was 45 GeV, showed that this estimate may be too low because 424 toponium states were found below the threshold for the creation of the bare top with angular momenta up to $L = 17$, the number of 3S_1 states was 12, and the separation between the S levels fell

from 946 MeV for the 2S–1S splitting to 80 MeV for the upper radial excitations. However, these riches will probably remain unattainable for a long time because the high-lying levels are difficult to separate, since the beams produced by the SLC and LEP accelerators have an energy spread¹⁰⁾ of a few tens of MeV (see Sec. 7 for further details). Thus, at any rate during the initial stages, one can hope only for the identification of the low-lying states, and we shall therefore confine our attention to these states, especially since, in many respects, they determine the basic physical conclusions, and the predictions of different potential models differ particularly sharply precisely for these states. Detailed spectroscopic tables for toponium can be found, for example, in Refs. 17, 34, 35, and 60–63.

Basic information on the behavior of the potential at short distances will be obtained once the masses and leptonic widths of the 1S–2S levels and the position of the 1P level have been determined.¹¹⁾ The leptonic width can be calculated theoretically from (27) (see below), in which the wave function at the origin, determined by solving the Schrödinger equation for a given potential, plays a significant role. We shall examine a number of cases (see Fig. 2), including the quasilogarithmic Martin potential³⁷ (12) with $\varepsilon \approx 0.1$, the Richardson potential^{32–34} R , which is an interpolation between the asymptotically free and linear confining contributions, and the potential BD with a “step,”⁵³ which takes into account the abrupt transition from current quarks with asymptotically free interaction to constituent quarks with nonperturbative interaction described phenomenologically. The three types of potential shown in Fig. 2 lead to significantly different predictions for the mass difference between the 2S and 1S levels (Fig. 3) and the leptonic widths of these levels (Fig. 4). It is clear that the difference between the predicted splitting can be up to almost 500 MeV, while leptonic widths differ by a factor of about five. There are also noticeable differences between the ratios of leptonic widths obtained for the 2S and 1S levels. The results of these extensive calculations can be generalized in the form of the following simple mnemonics:

- (1) large splitting (~ 900 MeV), large leptonic width of the 1S level (~ 6 keV), and small ratio of the leptonic widths in the 2S and 1S states (~ 0.25 – 0.3) are typical for asymptotically free monotonic potentials (R)
- (2) small splitting (~ 500 MeV), small leptonic width

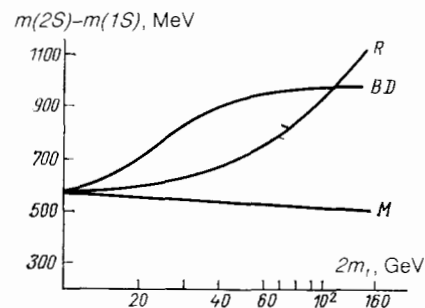


FIG. 3. Mass difference between the 2S- and 1S-levels as a function of twice the mass of the top quark for the three potentials, shown in Fig. 2.

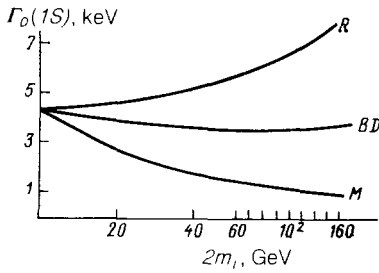


FIG. 4. Leptonic width of the 1S-state (without the Z^0 contribution) as a function of twice the mass of the top quark for the three potentials shown in Fig. 2.

(~ 1 keV), and a large ratio of leptonic widths ($\sim 0.5-0.55$) are typical for quasilogarithmic potentials (M)

(3) large splitting (~ 900 MeV), intermediate leptonic width of 1S levels (~ 3.5 keV), and large leptonic-width ratio ($\sim 0.5-0.55$) are typical for potentials with a "step" (BD).

Further important information can be deduced by measuring the position of 1P levels. Their "center of gravity" is shifted slightly relative to the 2S level, both in the asymptotically free monotonic potential and the quasilogarithmic potential (~ 100 MeV), whereas the potential with the step predicts a much greater splitting (~ 300 MeV).¹²⁾ In the first case, it will be possible to detect the 1P level using the $\theta' \rightarrow \gamma\chi_1$ radiative transition, but only if the mass of toponium is less than 90 GeV (see below). In the case of the potential with the step, the width of this decay [proportional to the cube of the photon frequency, ω^3 ; see (39)] will account for an appreciable fraction of the total width (tens of percent), and the transition will be clearly seen.

We note, in passing, that, if the 1P and Z^0 turn out to be practically degenerate with respect to the masses, we shall have the exotic possibility^{20,62)} of direct creation of the 1P resonance due to the axial vector coupling of the Z^0 (see Sec. 7).

It would therefore appear that the very earliest studies of the relative disposition of the 1S, 2S and 1P levels of toponium and of their leptonic widths will result in an elucidation of the asymptotic freedom parameters and of the transition from constituent to current quarks.

The asymptotically free part of the potential now plays a more important part and, therefore, all the data will be sensitive to the parameter Λ_{QCD} . A reduction in this parameter leads to a reduction in the derivative of the potential [see (20)], and hence to a reduction in the predicted leptonic width [see (11)] and level splitting. In the case of monotonic potentials, this type of change in Λ_{QCD} presents no real danger. This is so because it immediately affects the agreement with the data on charmonium and bottomium, which, for the commonly employed interpolations, are described with Λ_{MS} above 300 MeV. If it turns out that toponium spectroscopy leads to lower values of Λ_{MS} , we may be forced to use special interpolations, such as that proposed in Ref. 64, where an abrupt jump in the β -function was introduced,¹³⁾ this function being defined as the logarithmic de-

rivative of the color charge α_s with respect to the logarithmic of the transferred momentum q^2 :

$$\beta(\alpha_s) = \frac{d\alpha_s(q^2)}{d \ln q^2}. \quad (23)$$

In any case, the parameter Λ_{MS} used in the phenomenological approach is related to the absolute normalization of the potential and the quark masses.³⁴ Moreover, it must always be remembered that Λ_{MS} is related to the potential cutoff parameters Λ_m and Λ_c [see (20)] in momentum and coordinate spaces. These relationships were deduced in Refs. 33 and 65:

$$\ln \frac{\Lambda_m}{\Lambda_{\text{MS}}} = \frac{3}{2(33-2n_f)} \left(\frac{124}{27} - \frac{10}{9} n_f \right), \quad (24)$$

and in Refs. 45 and 66 [see (20)]:

$$\Lambda_c = e^C \Lambda_{\text{MS}}, \quad (25)$$

where $C = 0.5772 \dots$ is the Euler constant.

A more detailed discussion of possible determinations of Λ_{MS} in the case of monotonic interpolation of the potential can be found in the review paper in Ref. 67.

If spectroscopic data on low-lying levels of toponium were to confirm the necessity for a mass jump in the potential, the situation would be both more interesting and more definite because it is already clear from the hadronic width of toponium that QCD with $\Lambda_{\text{MS}} \approx 100$ MeV is valid at short distances. More accurate determinations of Λ_{MS} will depend on the details of the transition from current to constituent quarks, i.e., the parameter in the perturbative approach will be related to the nonperturbative mass jump.

The size of the high-lying radial excitations of toponium will be comparable with the size of bottomium and charmonium (0.3–0.8 fm), and will therefore serve as a good additional verification of the hypothesis that the potential is independent of quark flavor, although, as noted above, their identification and detection will be limited in practice by the energy spread in the colliding beams.

The same difficulties will arise in attempts to examine fine and hyperfine level splitting. In spite of all the ambiguities of the treatment of spin-orbit and spin-spin interactions, the splitting is predicted to be of the order of 10 MeV in the case of toponium and, therefore, once again, we have the problem of the beam energy spread.¹⁴⁾ Both these effects are relativistic and must, at the very least, be smaller than in the case of bottomium. The splitting is proportional to the square of the quark velocity and, according to estimates based on (14), it should decrease by almost an order of magnitude between bottomium and toponium in the case of the quasilogarithmic potential (i.e., up to 5 MeV). However, an appreciably smaller reduction is expected for more reasonable estimates using different mass dependences in (14). Nevertheless, the fine splitting can hardly be greater than 20 MeV. The precision with which this splitting can be estimated is related to the problem of separating the potential into the Lorentz-vector and Lorentz-scalar parts.⁵⁰⁾ This also applies to the inclusion of spin-spin interactions which govern the hyperfine splitting, although to a somewhat lesser extent because the spin-spin interactions are regarded as having a

shorter range. Usually, this splitting is estimated from the formula⁶⁸

$$\Delta E_{ss} = \frac{8\alpha_s}{9} \frac{|R_\theta(0)|^2}{m_\theta^3}, \quad (26)$$

which is obtained from the δ -function contribution due to the Laplacian of the Coulomb potential.¹⁵⁾ However, this formula is known to lead to estimates that are too high because real quarkonium potentials are less singular at the origin. Nevertheless, even in this case, the hyperfine splitting in toponium is no more than 20–40 MeV.^{20,50} Although it is small, we must emphasize that the difference between toponium and bottomium families is not very large in this context¹⁶⁾ [this is also indicated by qualitative estimates based on (19)].

We may therefore expect that toponium spectroscopy will confirm the expected validity of the usual nonrelativistic approach, the property of asymptotic freedom, the transition from current to constituent quarks, and the fact that the potential is quark-flavor independent.

From the QCD point of view, spectroscopic studies of toponium are expected to yield information on the role of nonperturbative effects, in particular, the ratio of long-wave^{69–71} to short-wave^{72–74} vacuum fluctuations during the phase transition between current to constituent quarks, and may suggest possible modifications of calculated levels of heavy quarkonium^{71–75} when this transition is taken into account in the case of the quasi-Coulomb interaction at short distances.

6. TOPONIUM DECAY MODES

6.1. General information

If the mass of toponium turns out, as expected, to lie between 60 and 120 GeV, its decays will be governed by weak, electromagnetic, and strong interactions in equal proportions (Refs. 14, 15, 19, 20, 23, 35, 62, 63, 76–78). This is the first time that we have encountered a situation in which all three types of interaction play more or less the same role in the decay of a bound hadronic system.

Decay can occur (1) as a result of quark annihilation, either direct (Figs. 5a–c) or through W-boson exchange (Fig. 5d); (2) as the decay of one of the quarks (Figs. 5e and f); and (3) during a hadronic (Fig. 5g) or radiative (Fig. 5d) transition to a lower lying state of toponium.

Moreover, toponium decay can be accompanied by the

creation of the supersymmetric partners of ordinary particles if their masses are low enough for such decays to be energetically possible. We shall examine them separately in Sec. 6.4.

The widths of all the annihilation decays of S-levels are proportional to the probability that the quark and antiquark will meet at the same point, i.e., to the square of the wave function of the system at zero relative separation between the quarks making up the system.¹⁷⁾ This probability can be obtained directly by solving the Schrödinger equation for a given model potential. It is sensitive to the shape of the potential and is actually the main nonperturbative element in the calculation of annihilation widths. The ratios of the widths of different annihilation channels corresponding to a given level do not depend on the wave function and can be calculated from perturbation theory. This is why it is common to quote the ratio of the width of a particular channel to the leptonic width of a given state (without taking into account the Z^0 boson exchange of Fig. 5a) calculated from the well-known formula^{79,80}

$$\begin{aligned} \Gamma(\theta \rightarrow l^+l^-) &= \Gamma_0(\theta) \left[1 - \frac{16}{3\pi} \alpha_s(m_\theta) \right] \\ &= \frac{16\alpha^2}{9m_\theta^2} |R_\theta(0)|^2 \left(1 - \frac{16}{3\pi} \alpha_s(m_\theta) \right). \end{aligned} \quad (27)$$

More precisely, it is common to consider the ratios

$$r_i = \frac{\Gamma_i}{\Gamma_0(\theta)}, \quad (28)$$

which do not include chromodynamic radiative corrections (see Appendix) because, on the one hand, they should be small in the toponium region, where $\alpha_s \sim 0.1$, and, on the other hand, they have still not been calculated for quark decays.

The predictions of different potential models for $\Gamma_0(\theta)$ were discussed in the last Section, where it was seen that the most realistic values of this quantity ranged from 3 to 6 keV (for $m_\theta \sim 70$ –80 GeV).

Let us begin with the physically most interesting case, namely, the creation of a neutral Higgs boson and a photon (Fig. 5c).⁸¹ In the standard model,

$$r_{H^0\gamma} = \frac{1}{2x} \frac{m_\theta^2}{m_W^2} \left(1 - \frac{m_{H^0}^2}{m_\theta^2} \right), \quad (29)$$

where $x = 4 \sin^2 \theta_w$ and θ_w is the Weinberg angle. It is clear that this decay width is not very different from the leptonic

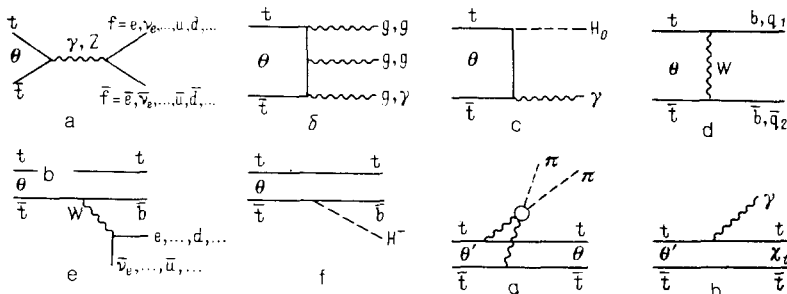


FIG. 5. Toponium decay diagrams: a–d—annihilation decays, e–f—individual quark decays and transitions between different states of toponium (g—hadronic, a—radiative).

width if the mass of toponium is close to the mass of the W boson, and the mass of the Higgs boson is not too close to that of toponium. Hence, for $m_{H^0} \lesssim 0.7m_\theta - 0.9m_\theta$, there is a very high probability of finding the neutral Higgs boson among the toponium decay products. This would be exceedingly important for the standard model of the electroweak interaction.

There are very simple formulas for the hadronic decay into three gluons and into two gluons and a photon (Fig. 5b). These modes have played an important part in charmonium and bottomium decays. These formulas are⁶

$$r_{ggg} = \frac{5(\pi^2 - 9)}{18\pi} \frac{\alpha_s^3}{\alpha^2}, \quad (30)$$

$$r_{gg\gamma} = \frac{8(\pi^2 - 9)}{9\pi} \frac{\alpha_s^2}{\alpha}, \quad (31)$$

and lead to the simple result

$$\frac{\Gamma_{gg\gamma}}{\Gamma_{ggg}} = \frac{16\alpha}{5\alpha_s}. \quad (32)$$

As can be seen, measurement of these ratios is important for the determination of the color interaction constant α_s . Although the three-gluon width turns out to be actually somewhat greater than the leptonic width (outside the Z^0 region), the situation is now different from that of charmonium and bottomium because this width does not now provide the principal contribution to the toponium width, which is mainly due to the annihilation decay with the creation of the fermion-antifermion pair $f\bar{f}$ (Figs. 5a and d for the $b\bar{b}$ pair) and the decay of a single quark (Fig. 5e). The corresponding ratios (28) can be written in the form^{23,78,82}

$$r_{f\bar{f}} = \frac{c_f}{e_f^2} \left\{ e_f^2 e_{f'}^2 + 2 \frac{e_f e_{f'} v_f v_{f'}}{y^2} \operatorname{Re} x_z + \frac{v_f^2 (v_f^2 + 1)}{y^4} |x_z|^2 + \delta_{f,b} \left[\frac{v_f (1 - v_f)}{3xy^2} x_W \operatorname{Re} x_z - \frac{e_f e_{f'}}{3x} x_W + \frac{x_W^2}{18x^2} \right] \right\}, \quad (33)$$

where

$$\begin{aligned} x &= 4 \sin^2 \theta_W, & y &= 2 \sin 2\theta_W, \\ x_z &= \frac{m^2}{m^2 - m_Z^2 + i\Gamma_Z m_Z}, & x_W &= \frac{m^2}{m_W^2} \frac{m_W^2 + (m^2/8)}{m_W^2 + (m^2/4)}, \\ c_f &= \begin{cases} 3 & \text{for quarks} \\ 1 & \text{for leptons} \end{cases}, & \delta_{f,b} &= \begin{cases} 1, & f=b, \\ 0, & f \neq b, \end{cases} \\ e_u = e_c = e_t &= \frac{2}{3}, & e_d = e_s = e_b &= -\frac{1}{3}, \\ e_{\nu_e} = e_{\nu_\mu}^{\nu_e} = e_{\nu_\tau} &= 0, & e_e = e_\mu = e_\tau &= -1, \\ v_u = v_c = v_t &= 1 - \frac{2}{3} x, & v_d = v_s = v_b &= -1 + \frac{1}{3} x, \\ v_{\nu_e} = v_{\nu_\mu} = v_{\nu_\tau} &= 1, & v_e = v_\mu = v_\tau &= -1 + x. \end{aligned}$$

We note that, in (33), we have neglected all charged-current contributions, which are suppressed by the Cabibbo angle.

Of the two-fermion decays, the decays into a neutrino and an antineutrino are of particular interest because they may indicate the number of types of neutrino (see Sec. 6.5).

The β -decay of a single quark (Fig. 5e) does not require the annihilation process, so that $\Gamma_0(\theta)$ remains explicitly in (28).⁸³

$$r_t = \frac{3}{32\pi^3} \frac{G_F^2 m_t^6}{\Gamma_0(\theta)} f(\rho, \nu), \quad (34)$$

where $\rho = m_t^2/m_W^2$, $\nu = m_b^2/m_t^2$ and

$$0.9 < f(\rho, \nu) \approx \frac{2}{\rho^4} (1 - 8\nu) \{ 6[\rho + (1 - \rho) \ln(1 - \rho)] - 3\rho^2 - \rho^3 \} < 1.3$$

for $30 \text{ GeV} < m_t < 55 \text{ GeV}$.

This width increases rapidly with increasing quark mass, and is practically always appreciably greater than the leptonic width.

There is the interesting, though not highly probable,¹⁸⁾ possibility that toponium will decay wholly along the channel involving the creation of charged scalar Higgs particles (if such particles exist) with masses less than the mass of toponium. In that case,

$$r_{H^\pm} = \frac{G_F |V_{tb}|^2}{4\sqrt{2}\pi} \frac{m_t^3}{\Gamma_0(\theta)} \left(1 - \frac{m_{H^\pm}^2}{m_t^2} \right)^2, \quad (35)$$

i.e., this channel width exceeds the leptonic width by 3–4 orders of magnitude for $m_{H^\pm} < 0.9m_t$ and increases rapidly with increasing toponium mass. (In this estimate, we have, of course, assumed that $|V_{tb}|^2 \sim 1$.)

Other possible decays are those in which a top quark transforms into a d- or s-quark by W-meson exchange (Fig. 5d with q_1 and q_2) or by direct creation of the W-meson [if the mass of the top quark exceeds the mass of the d(s)-quark plus the mass of the W-meson]. However, the probabilities of these decays are low because the off-diagonal elements of the Kobayashi-Maskawa matrix V_{tq} with $q = d$ or s are small.¹⁹⁾ They are given by

$$r_{q_1 q_2} = \frac{3|V_{tq_1} V_{tq_2}|^2}{4x^2} x_W^2, \quad (36)$$

$$r_{qW} = \frac{G_F |V_{tq}|^2}{4\sqrt{2}\pi\Gamma_0(\theta)} m_t^3 \left(1 + 2 \frac{m_W^2}{m_t^2} \right) \left(1 - \frac{m_W^2}{m_t^2} \right)^2. \quad (37)$$

Of course, if these decays were to be detected, they would provide a way of measuring the off-diagonal elements of the Kobayashi-Maskawa matrix.

Figure 6 shows²³ the width of the different decay channels of the ground state of toponium as functions of its mass, based on estimates provided by (27) and (37) for the following parameter values:

$$\left. \begin{aligned} \Gamma_0(\theta) &= 5 \text{ keV}, & m_W &= 83.2 \text{ GeV}, & m_Z &= 94.0 \text{ GeV}, \\ \sin^2 \theta_W &= 0.217, & \Gamma_Z &= 2.5 \text{ GeV}, \\ \alpha_s(m) &= \frac{12\pi}{23 \ln(m/100 \text{ MeV})^2} & (n_f &= 5). \end{aligned} \right\} \quad (38)$$

Decays into fermion-antifermion pairs and decays of a single top quark are seen to predominate.

The decays of the higher-lying radial excitations are described by the same formulas, but the square of the wave function at the origin is then usually smaller, so that the role of annihilation channels is reduced and that of the single-quark decay is greater. Moreover, there are two further pos-

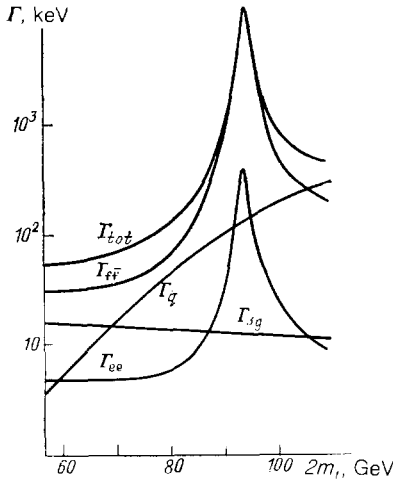


FIG. 6. Total decay width of the 1S-state of toponium and its decay width for the individual channels as functions of twice the mass of the top quark.

sibilities for transitions to lower-lying states, namely, the hadronic (Fig. 5g) and radiative (Fig. 5h) channels. In the case of toponium, the hadronic channel is highly suppressed as compared with charmonium and bottomium, and estimates^{85,86} show that its contribution to the total width is no more than 1 keV (most likely, about 0.5 keV), so that it can be practically ignored²⁰⁾ (since the total 2S widths will not be less than 80 keV). The contribution of radiative decays has a significant dependence on the shape of the potential and on the splitting of the 2S–1P levels (already discussed in Secs. 4 and 5). The width of the $\theta' \rightarrow \gamma\chi_t$ transition²¹⁾ can be written in the form⁶²

$$\begin{aligned} \Gamma(\theta' \rightarrow \gamma\chi_t) &= \frac{16}{27} \alpha \omega^3 M_{21}^2 \\ &\approx \left(\frac{45 \text{ GeV}}{m_t}\right)^{1,25} \left(\frac{\omega}{100 \text{ MeV}}\right)^3 (\text{keV}), \end{aligned} \quad (39)$$

where

$$M_{21} = \int_0^\infty r^3 R_2(r) R_1(r) dr \quad (40)$$

is the dipole matrix element and ω is the frequency of the γ -ray (approximately equal to the 2S–1P splitting). This width increases as the cube of the level separation and appreciably decreases with increasing mass of the top quark. Its contribution to the total width is found to be 2–5% for $m(\theta') - m(\chi_t) \approx 100 \text{ MeV}$ (monotonic interpolations) or 30% for $m(\theta') - m(\chi_t) \approx 300 \text{ MeV}$ (potential with a step and $30 < m_t < 40 \text{ GeV}$). Naturally, the fraction of decays along this channel decreases rapidly in the Z^0 region.

Let us now consider the decay width for the 2S(θ') and 1S(θ) states of toponium. If we neglect the small mass difference between θ and θ' , the ratios of all the annihilation decay widths will be the same and equal to the ratio of the squares of the wave functions in these states for zero relative separation between the quark and antiquark:

$$\frac{\Gamma_{\text{ann}}(\theta')}{\Gamma_{\text{ann}}(\theta)} \approx \frac{|R_{\theta'}(0)|^2}{|R_\theta(0)|^2} \approx 0.3 - 0.5. \quad (41)$$

[In particular, $\Gamma_0(\theta') \approx (0.3-0.5)\Gamma_0(\theta)$.] The first figure in (41) is obtained by monotonic interpolation of the potential with $\Lambda_{\text{MS}} \approx 500-400 \text{ MeV}$, and the second for the step interpolation with $\Lambda_{\text{MS}} = 100 \text{ MeV}$ (and for quasilogarithmic potentials).

For the single-quark decays, the width is practically independent of the number of radial excitations, so that

$$\frac{\Gamma_t(\theta')}{\Gamma_t(\theta)} \approx 1. \quad (42)$$

We may therefore conclude that the relative fractions of annihilation channels will be appreciably lower for θ' than for θ , the relative contribution of single-quark decays will increase, and, possibly, there will be an appreciable contribution due to the radiative transition to χ_t . For higher-lying radial excitations of toponium, this tendency for an increase in the relative contribution of single-quark decays is more pronounced.

The $\chi_t \rightarrow \gamma\theta$ radiative decay widths depend on the shape of the potential, but it may be considered that they do not exceed 130 keV (see Refs. 54 and 76). The decay of the χ_t will divide equally between the radiative transition to the θ and a weak decay to the top quark.

We emphasize that the decay channel ratio of toponium will vary significantly with varying mass (Fig. 6). Processes involving the creation of a quark-antiquark pair, three-gluon decays, and weak decays of the top quark are important up to 85 GeV. Near the Z^0 -boson ($85 < m < 105 \text{ GeV}$), there is a rapid increase in the part played by decays into fermion-antifermion pairs. While the quarks continue to play a dominant role, the interesting process of neutrino-antineutrino pair production begins to provide an important contribution. Weak decays of the two quark become dominant for high masses. This leads to an appreciable broadening and smoothing out of resonances. Moreover, transitions from radially excited S-states to states with other L become so rare that it is unrealistic to speak of toponium spectroscopy in this region.

6.2. Scalar Higgs particles

The situation with scalar particles is one of the most intriguing in particle physics. They are welcome guests in theory, but elusive spirits in experiment. It may be that toponium will be the first to reveal the last element of modern gauge theories of electroweak interactions that has not yet been found experimentally, namely, the scalar Higgs particle. This particle ensures the breaking of the symmetry of electroweak interactions and is responsible for the mass of known particles.

In the minimal standard Weinberg-Glashow-Salam model there is only the one neutral Higgs particle H^0 . In nonminimal models (models with technicolor, supersymmetry, and so on), there is a set of neutral and charged scalar fields.⁵⁷ However, in neither case has theory been able to predict the masses of these particles (although it does provide certain limits for them). We can only hope that, if the scalar particles are not too massive ($m_H < m_\theta$), they will manifest themselves in toponium decays. In particular, a heavy enough toponium will be of particular interest because

the strength of coupling between the Higgs particles and fermions is usually assumed to be proportional to the mass of the fermion (quark or lepton). This means that the fraction of this channel in toponium is approximately 1–3%, i.e., greater by two orders of magnitude than for bottomium (and, moreover, for a broader range of mass), as can be clearly seen from (29). This reaction is readily detected by looking for the monochromatic photon, and the determination of the mass of the Higgs particle is then an elementary matter²²⁾ because this is a two-particle decay.

Estimates^{20,23,57} show that the statistics possible on the SLC and LEP accelerators will be good enough to detect this decay even if the H^0 mass accounts for 90% of the mass of toponium (tens or hundreds of events per 1000 working hours). It should not take more than a year to raise the upper limit for the H^0 mass to 65, 80, and 85 GeV if the mass of toponium turns out to be 70, 90, and 110 GeV, respectively.²³ The authors of the review paper in Ref. 23 have carried out a careful study of the possible signal-to-noise ratios and have concluded that toponium is an excellent object to look at in searches for heavy Higgs particles.²³⁾

As far as charged scalar Higgs particles are concerned, we have already noted above that the data obtained by the UA1 group² on the semileptonic decays of top quarks have practically excluded the possibility of their creation. If the opposite situation prevails, (35) shows that practically all the toponium decays should proceed with the creation of such particles.

6.3. Supersymmetric particles

The supersymmetric partners of ordinary particles constitute a fundamentally new element in physics. So far, they have been "seen" only "at the tip of the pen" (see the review papers in Refs. 19, 23, and 87-89). It is hoped that it will be possible to detect them experimentally in toponium decays, provided they exist and their masses are not too large. Unfortunately, theoretical predictions of these masses are different in different models and have had to be regarded as free parameters, so far.

As in ordinary toponium decays, the creation of supersymmetric particles can occur either as a result of the annihilation of a top quark and an antiquark, or by the decay of an individual quark. Let us consider the first possibility, assuming that these decay channels are kinematically accessible.

One of the channels for the creation of the gluino is the process shown in Fig. 7, in which one of the gluinos of Fig. 5b is virtual and transforms into a gluino pair.⁹⁰ This process is interesting in that the corresponding decay frictions depend only on the assumed gluino mass and are unrelated to any model parameters. Naturally, they decrease with increasing gluino mass, but the actual gluino mass range that has to be investigated with the aid of toponium is 4 to 10 GeV, so that a gluino lighter than 4 GeV would be created in bottomium decays, whereas a gluino of 10 to 40 GeV has already been excluded by collider data.^{91,92} However, even in this interval, the prospects for finding the gluino^{19,23} are not too encouraging:

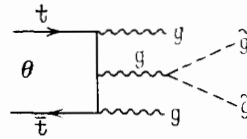


FIG. 7. Decay of the 1S-state of toponium with the creation of two gluons and two gluinos.

$$\begin{aligned} \text{Br}(\theta \rightarrow g\tilde{g}\tilde{g}) &\approx 10^{-2}, \\ \text{Br}(\theta' \rightarrow \gamma\chi_t \rightarrow g\tilde{g}) &\approx 10^{-3}, \end{aligned} \quad (43)$$

if the gluino mass is 5 GeV. If the potential with the step turns out to be valid, the situation is not much improved by higher $\theta' \rightarrow \gamma\chi_t$ transition probability. An overall reduction in the role played by three-gluon hadronic decay modes will affect the properties of toponium.

Moreover, since the Z^0 decay channel is preferred for the creation of gluinos with masses of this order, it seems unlikely that this toponium decay process (Fig. 7) will actually be used.

Other possibilities for gluino creation in toponium decays are found to depend on the particular models employed and on their parameters. For example, there would be considerable interest in the transformation of toponium into a pair of gluinos as a result of the exchange of the scalar partner of the top quark (Fig. 8). This so-called "stop quark" is found in a number of models to be the lightest of all the scalar quarks with mass approaching that of the top quark. The selection rules in this process are such that decays from all states are possible if the masses of the scalar partners of quarks with right and left helicities are different, but, if the masses are equal, only the decays of the χ_1 and η_1 are admissible. For us, the important point is that, in both cases, the decays of these states into a gluino pair turn out to be very significant^{19,23,93-95} or even dominant.

For example, the ratio of the two-gluino toponium decay width to the leptonic width is given by

$$r(\theta \rightarrow \tilde{g}\tilde{g}) = \frac{3}{2} \left(\frac{\alpha_s}{\alpha}\right)^2 \left(\frac{m_{\tilde{g}}}{m_{\theta}}\right)^2 \quad (44)$$

when one of the scalar-quark masses is equal to the mass of the top quark and the other is much greater, where $m_{\tilde{g}}^2 \ll m_{\theta}^2$.

Since this decay channel produces a clear signal (two-particle channel with the creation of energetic gluinos), it is very attractive from the experimental point of view. Estimates show²³ that the background can be reliably disposed of and the mass of the gluino can be measured to better than ± 1 GeV.

A photino could be created in these processes instead of the gluino, but the probability of this is low and detection difficult.

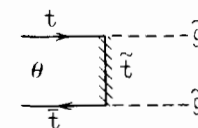


FIG. 8. Decay of toponium into a pair of gluinos as a result of scalar top-quark exchange.

The process $\theta \rightarrow \tilde{g}\tilde{g}$ with the participation of the photon⁹⁶ and proceeding by “stop-quark” exchange could be of interest. There is some hope for the detection of the gluino even if its mass is large (say, $m_{\tilde{g}} = 60$ GeV for $m_{\theta} = 80$ GeV). Such gluinos are appreciably more difficult to detect in Z^0 decays.

θ -decay channels such as $\tilde{H}\tilde{\gamma}, \tilde{Z}\tilde{\gamma}$ (Ref. 94), $\gamma\tilde{g}\tilde{g}$ (Ref. 96), $\tilde{g}\tilde{t}$, and $\gamma\lambda\lambda$ (Ref. 97), where λ represents a weakly-interacting Goldstone fermion,⁹⁸ seem to be less accessible to investigation.

A highly unlikely but intriguing possibility involves the decay of the top quark, which can occur if its mass exceeds the sum of the masses of the stop quark and the gluino. The decay width (see Fig. 9) is very large⁹³:

$$\Gamma = \frac{4}{3} \alpha_s m_t \left(\frac{2p_{\tilde{g}}}{m_t} \right)^2. \quad (45)$$

When the gluino momenta $p_{\tilde{g}}$ are not too small, this decay width may reach 1 GeV, i.e., it will exceed the level separation in the toponium system, and will thus destroy the entire resonance structure and destroy toponium physics as such. However, this possibility seems to have been eliminated by the observation of the semileptonic decays of top quarks by the UA1 collaboration.² The problem with the decay of the top quark will be finally resolved if mesons with bare top are observed in Z^0 decay. This will occur before toponium is found. Their influence on toponium will therefore be understood in advance.

Thus, although numerous modes have been proposed for the decay of toponium with the creation of supersymmetric partners of ordinary particles, the number of real candidates has been reduced by the first collider experiments, and the situation will rapidly become clear as soon as sufficient SLC statistics on mesons with bare and hidden top become available.

6.4. The structure of quarks and Λ_{QCD}

The transition from current to constituent quarks has already been examined in sufficient detail in Sec. 4. Here, we emphasize once again the importance of the field-theoretic understanding of the details of this phase transition, should it be discovered in toponium.

As emphasized earlier, its experimental manifestation would be large $\theta' - \theta$ and $\theta' - \chi_t$ level differences (and, hence, relatively large $\theta' \rightarrow \gamma\chi_t$ radiation transition widths), as well as a large ratio of θ' and θ leptonic widths. It seems to us that the real task for potential models in this case is not merely to determine Λ_{QCD} , but to investigate the nature of the phase transition. Indeed, it would be logical to adopt the

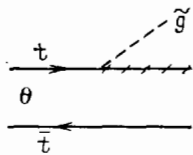


FIG. 9. Decay of the top quark in toponium into its scalar partner and a gluino.

scheme in which *only* asymptotically free interaction potentials between current quarks act at short distances with $\Lambda_{\text{QCD}} \approx 100$ MeV (determined from other data) whereas, at large distances, there is *only* the phenomenological interaction potential between the constituent quarks, which has been relatively well established from experimental data on charmonium and bottomium. Studies of the intermediate region and of its influence on the parameters of all three quarkonium families would then be a source of information, facilitating a better understanding of the quark phase transition.

Of course, the success of the entire program would also confirm the phenomenon of asymptotic freedom with a parametrization following from the QCD sum rule.

6.5. Number of types of neutrino

Toponium can be used³⁵ to determine the number of types of neutrino in nature, which is important for explaining the number of generations of leptons and quarks, for physical applications, and so on. This new method of counting the number of neutrinos can be used if we know the fraction of toponium decays along the neutrino channel (see Fig. 6). For example, for toponium of mass 80 GeV, we have

$$\frac{[\text{Br}(\nu\bar{\nu})]_{\text{for one type of } \nu}}{\text{Br}(\mu^+\mu^-)} \approx 0.7. \quad (46)$$

Thus, having measured the total probability of decays into neutrinos, we can determine the number of types of neutrino.

The problem is how to record this type of decay. First, we must have a specific trigger that would indicate that the decay has taken place. This can be done, for example, by using the photon.⁸⁴ In this method, we set the energy of the colliding electron-positron beams just above the mass of toponium and record the processes

$$e^+ + e^- \rightarrow \gamma + \theta \begin{cases} \rightarrow \gamma + \mu^+ + \mu^-, \\ \rightarrow \gamma + \text{missing mass}, \end{cases} \quad (47)$$

and identify toponium creation by examining the energy of the photon. The fractions of decays along these channels determine the number of types of neutrino. It is important to note, however, that an analogous procedure, using the creation of Z^0 rather than toponium, would be still more effective.

However, toponium can also be used with another trigger, for example, a pion pair, if we consider the processes

$$e^+ + e^- \rightarrow \theta' \rightarrow \pi^+ + \pi^- + \theta \begin{cases} \rightarrow \pi^+ + \pi^- + \mu^+ + \mu^-, \\ \rightarrow \pi^+ + \pi^- + \text{missing mass}, \end{cases} \quad (48)$$

discussed above (see Fig. 5g and the estimates in Sec. 6.1), where the missing mass is equal to the mass of the θ ; once again, we can estimate the number of types of neutrino.

The relative importance of decays into a neutrino pair becomes greater near the Z^0 . Their fraction approaches 10% when $m_{\theta} = 80$ GeV.

6.6. The Weinberg angle

Toponium can be used to determine the strength of coupling of a neutral current to a top quark and, consequently,

to determine the Weinberg angle because the vector part of the neutral current is determined by the constant

$$g_{\mathbf{v}, t} = \frac{2I_{3t} - e_t x}{y}, \quad (49)$$

where I_{3t} is the component of the isospin of the t-quark, and the other quantities are given by (33). We recall that $x = 4 \sin^2 \theta_w$ and $y = 2 \sin 2\theta_w$. As can be seen from (49), the quantity $g_{\mathbf{v}, t}$ can be used to determine independently the charge of the quark and its isospin. Using generally adopted notation, we find that

$$g_{\mathbf{v}, t} = \frac{v_t}{y} \quad (50)$$

and the determination of $g_{\mathbf{v}, t}$ is equivalent to finding the Weinberg angle.

We emphasize that toponium involves only the vector contribution of the neutral current, so that its use is preferred to, for example, the consideration of top-quark decays, for which the axial vector part must be included (and also QCD corrections and effects connected with the quark mass).

We have already seen from (33) that studies of the decay of toponium into a fermion-antifermion pair will, in themselves, provide information on the Weinberg angle, but high precision can hardly be expected.

Four methods have been proposed for a more accurate determination of the Weinberg angle, using the properties of toponium.^{19,23,63,78,83,99-104} Without going into detail, we shall describe the basic ideas and results. Detailed accounts can be found in the references just quoted.

The fundamentally new factor in the case of toponium is the large part played by the Z^0 boson in toponium creation and decay processes. This leads to appreciable effects in which parity conservation is violated. The proposed methods exploit these effects to a greater or lesser extent.

6.6.1. Decay of an individual quark^{83,104}

The angular distribution of leptons from semileptonic decays of quarks in toponium will exhibit a characteristic asymmetry even when the initial beams are unpolarized. The point is that the Z^0 boson ensures that toponium is created with a degree of longitudinal polarization, so that the component of its spin \mathbf{s} along the collision axis is given by

$$\langle \mathbf{s} \cdot \mathbf{n}_e \rangle = \alpha_{\text{RL}}^{\text{on}}, \quad (51)$$

where

$$\left. \begin{aligned} \alpha_{\text{RL}}^{\text{on}} &= -2 \frac{\text{Re}(\lambda^* \lambda')}{|\lambda|^2 + |\lambda'|^2}, \\ \lambda &= \frac{3}{2} \frac{v_e v_t}{y^2} \frac{m_\theta^2}{m_\theta^2 - m_Z^2 + i m_Z \Gamma_Z} - 1, \\ \lambda' &= -\frac{3}{2} \frac{v_t}{y^2} \frac{m_\theta^2}{m_\theta^2 - m_Z^2 + i m_Z \Gamma_Z} \end{aligned} \right\} \quad (52)$$

(the superscript "on" indicates that only the resonance contribution is taken into account; the subscripts RL are explained in Sec. 6.6.4., below).

Consequently, the quarks in toponium are also polarized, and the parity-violating term ensures that the leptons

produced in the decay have an asymmetric angular distribution²⁴⁾:

$$dN \sim (1 + \mathbf{n} \cdot \mathbf{s}) d\Omega \sim \left(1 \pm \frac{3}{4} \alpha_{\text{RL}} \cos \theta\right) d(\cos \theta), \quad (53)$$

where the two signs correspond to the lepton charges. The quantity α_{RL} is obtained by averaging the resonance (σ^{R}) and background (σ^{B}) contributions:

$$\alpha_{\text{RL}} = \frac{\alpha_{\text{RL}}^{\text{on}} \sigma^{\text{R}} + \alpha_{\text{RL}}^{\text{off}} \sigma^{\text{B}}}{\sigma^{\text{R}} + \sigma^{\text{B}}}. \quad (54)$$

The formula for the background $\alpha_{\text{RL}}^{\text{off}}$ will not be reproduced here (see Ref. 23). The high probability of decay along this channel, the presence of a single hard lepton, and the low background render this reaction very attractive for the determination of α_{RL} and, consequently, of the Weinberg angle [using (52)].

6.6.2. Energy spectrum of hadrons from τ -lepton decays^{101,102,105}

Another effect that is linear in the vector component of the neutral current can be seen in the energy spectrum of hadrons (pions or ρ -mesons) from the decay of τ -leptons (for example, $\tau \rightarrow \pi \nu$) created in e^+e^- -collisions in accordance with the processes of Fig. 5a. Unpolarized τ -leptons naturally lead to a flat hadron energy spectrum. The neutral current then ensures that the polarization of the τ -leptons is proportional to α_{RL} and, hence, the energy spectrum is asymmetric and includes a linear term that is proportional to α_{RL} and has different signs on the left- and right-hand halves of the spectrum. This enables us to determine the sign of $g_{\mathbf{v}, t}$ as well. Unfortunately, there are practical difficulties connected with the fact that the fraction of decays along the corresponding channels is small.

6.6.3. Forward-backward asymmetry of leptons and jets^{66,77,78}

An effect quadratic in $g_{\mathbf{v}, t}$ (or α_{RL}) can be observed in the form of the forward-backward asymmetry of leptons and quark jets produced in accordance with the annihilation diagram of Fig. 5a, where the asymmetry in the region of the resonance is significantly different from that outside resonance (in the continuum). Of course, this effect actually appears only when the mass of toponium is close enough to that of the Z^0 boson. The angular distribution of an arbitrary fermion-antifermion pair can be written in the form:

$$\frac{dN}{d(\cos \theta)} \sim 1 + \cos^2 \theta + 2\alpha_{\text{FB}} \cos \theta, \quad (55)$$

where, in the case of leptons, we have in the toponium region

$$\alpha_{\text{FB}}^{\text{on}} = \alpha_{\text{RL}}^2. \quad (56)$$

The asymmetry of the muon pairs at maximum θ is shown in Fig. 10 as a function of m_θ for the resonance (on) and continuum (off) contributions.⁶³ As can be seen, the two are very different. Problems involved in accounting for the mixture of resonance and continuum, the energy spread of the primary beams, and the luminosity of the accelerators are discussed in Ref. 23, where it is concluded that, during the first working year of the LEP accelerator, the quantity α_{RL}

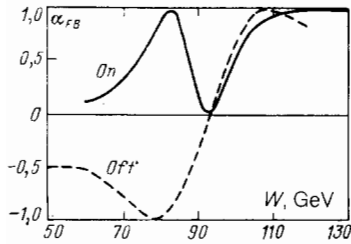


FIG. 10. Forward-backward asymmetry of the μ^- from the $\theta \rightarrow \mu^+ \mu^-$ decay at maximum θ (on), and of the background events (off), for different masses of the toponium.⁶³

will be determined to within 0.1 and, later, to within 0.05, so that, in the latter case, $\sin^2 \theta_w$ will be determined to within 4×10^{-3} .

A similar analysis can be performed for the quark jets (Fig. 5a).

We mention one further possibility, namely, the asymmetry in the annihilation of toponium into a $b\bar{b}$ pair due to W-boson exchange (Fig. 5d), which can provide information on charged currents.

6.6.4. Polarized beams^{63,78,99,100}

The neutral current contribution should manifest itself directly when the colliding electron-positron beams are polarized. Although polarized beams can hardly be achieved in the near future on the SLC and LEP accelerators, studies of such processes are interesting from the fundamental point of view and, moreover, show their interrelation with the effects investigated above for unpolarized particles.

The fermion-antifermion production cross sections for longitudinally polarized beams must be different for different (right and left) polarizations. The polarization asymmetry is defined by

$$\alpha_{RL} = \frac{\sigma_R - \sigma_L}{\sigma_R + \sigma_L}, \quad (57)$$

where σ_{RL} is the production cross section for right (R) and left (L) beam polarizations. This quantity appears in the coefficients in the above formulas for unpolarized beams. As already noted, it is different for the resonance contribution and for the continuum, and its weighted mean can be obtained from (54). In the case of the $\mu^+ \mu^-$ pair production process, the resonance contribution to the polarization asymmetry at maximum θ is shown in Fig. 11 as a function of toponium mass and is compared with the background.

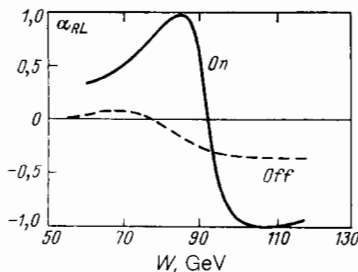


FIG. 11. Polarization asymmetry at maximum θ (on), and of background events (off), as a function of the toponium mass.⁶³

It is clear that the two distributions are very different. We also note that, in the case of a transversely polarized beam, the azimuthal distributions of the pairs should be different in the resonance region and outside this region.⁶³

Thus, all the effects considered above can be used to measure α_{RL} and, hence, the neutral current coupling constant $g_{V,\mu}$, i.e., the Weinberg angle, can be determined (see (50)). The precision of such measurements should be higher than that achieved by other methods at present.²³

6.7. Interference of toponium and the Z^0 -bosons¹⁰⁶⁻¹¹⁰

If the mass of toponium turns out to be close to that of the Z^0 -boson, there will be a significant change in the ratio of the toponium decay channels and an appreciable increase in its width (see Fig. 6). Moreover, there is also a very interesting interference effect between toponium and the Z^0 -boson which is well defined if the toponium family falls into the region of the Z^0 -boson peak. In particular, if, for example, the mass of toponium is exactly equal to that of the Z^0 -boson, not only will the increase in the cross-section peak not appear, but, on the contrary, there will be a very narrow dip down to zero.

The physical origin of this specific interference pattern can be readily understood by considering, for example, the contribution of toponium to the total cross section for the creation of the muon pair. The entire specificity of this case depends on the phase difference between the amplitudes for processes with the exchange of a virtual photon and the exchange of a virtual Z^0 -boson. While, in the first case, the amplitude is always real, in the second, it is purely imaginary for energies near the mass of the Z^0 -boson (as for any resonance), but is very nearly real well away from the resonance. At the same time, the contribution of toponium to the amplitude for the process is always purely imaginary at the point of maximum $s = m_\theta^2$. Hence, if toponium lies well away from the Z^0 -boson, it provides an imaginary term that has to be added to the real amplitude, i.e., it produces an additive contribution to the total cross section for the process. If, on the other hand, toponium lies near the Z^0 -boson, both contributions to the amplitude will be purely imaginary and opposite in sign, i.e., we have cancellation of amplitudes and, hence, the dip in the total cross section.

All that we have said above can be readily demonstrated by writing down the contributions of the diagrams of Figs. 12a and b for the two limiting cases $m_\theta \ll m_Z$ and $m_\theta = m_Z$. In the former case, $s = m_\theta^2 \ll m_Z^2$ and we have

$$A(m_\theta) \sim \frac{1}{m_\theta^2} + \frac{1}{m_\theta^2} \frac{g_{\theta\gamma}^2}{im_\theta\Gamma_\theta} \frac{1}{m_\theta^2} \equiv A_{B,\gamma} - iA_\theta, \quad (58)$$

i.e.,

$$|A(m_\theta)|^2 \sim A_{B,\gamma}^2(m_\theta) + A_\theta^2(m_\theta), \quad (59)$$

which means that toponium enhances the photon contribution to the cross section for the process when the Z^0 contribution is small.

When $s = m_\theta^2 = m_Z^2$, we have

$$A(m_\theta) \sim \frac{1}{im_\theta\Gamma_Z} + \frac{1}{im_\theta\Gamma_Z} \frac{g_{\theta Z}^2}{im_\theta\Gamma_\theta} \frac{1}{im_\theta\Gamma_Z} \equiv -iA_{B,Z} + iA_\theta, \quad (60)$$

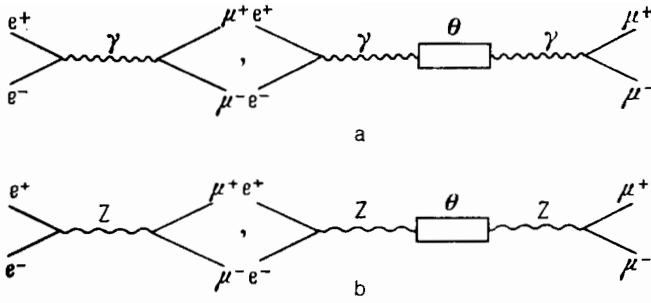


FIG. 12. The γ - θ interference (a) and the Z - θ interference (b) in the $e^+e^- \rightarrow \mu^+\mu^-$ process.

which shows that we have completely destructive interference between Z^0 and θ (the contribution of the photon is then small):

$$|A(m_\theta)|^2 \sim (A_{B,Z}(m_\theta) - A_\theta(m_\theta))^2 = 0, \quad (61)$$

since

$$g_{\theta Z}^2 = m_\theta^2 \Gamma_\theta \Gamma_Z. \quad (62)$$

Detailed calculations, taking into account all the resonances of the toponium family, lead to the interference pattern shown in Fig. 13. However, it will be impossible to observe this structure in practice because of the energy spread of the primary beam, which is usually about 0.1%, i.e., of the order of 50 MeV in the case of SLC and LEP. Averaging over an energy spread of this size will smooth out the interference pattern and, instead of the peaks and dips, we shall have only an indication of structure (Fig. 14), which will be resolvable only when good enough experimental statistics become available.

The closeness of toponium to the Z^0 -boson (for $|m_\theta - m_Z| \lesssim \Gamma_Z$) may affect not only the decay modes, but also physical parameters such as the mass and width of resonances.¹⁰⁶⁻¹⁰⁸ A sharp increase in the toponium decay width is clearly seen in Fig. 6. The shift of the Z^0 -boson mass may amount to 3-4 MeV,²⁰ which is hardly measurable.

7. PRODUCTION OF TOPONIUM

So far, our discussion has proceeded as if we already had a set of well-defined toponium production events without

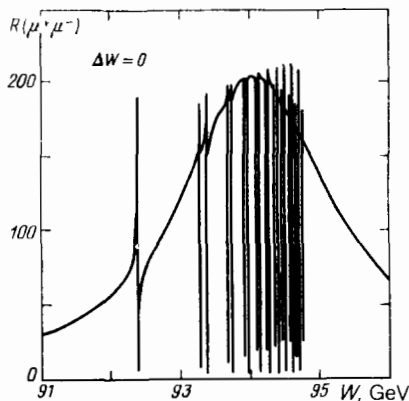


FIG. 13. $R(\mu^+\mu^-)$ for a top quark of mass 47 GeV (Ref. 63).

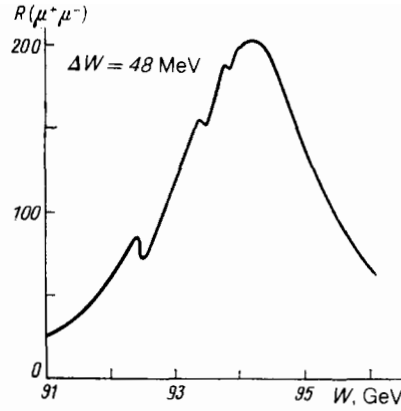


FIG. 14. $R(\mu^+\mu^-)$ for a top quark mass of 47 GeV, averaged over the beam energy spread with $\Delta W = 48 \text{ MeV}$ (Ref. 63).

any background events. The educated pessimist will, of course, point out that, as the mass of a resonance increases, the signal-to-noise ratio will rapidly decrease because of the energy spread of the beam (as already verified for the transition from charmonium to bottomium), so that we have to face the problem of identifying the toponium events. The optimist will reply^{18,20,23} that, although the number of background events will actually be comparable with (or may be even greater than) the number of toponium events, the total number of events will be large enough to separate the two within a reasonable interval of time and, hence, to enable us to investigate the physics of toponium.

The question is: is this conclusion well founded? The design luminosity of the SLC (average) and LEP (maximum) is, respectively, $L_0 = 6 \times 10^{30} \text{ cm}^{-2}\text{s}^{-1}$ and $L_m = 2 \times 10^{31} \text{ cm}^{-2}\text{s}^{-1}$ (outside the Z^0 peak). However, for technical reasons, the mean luminosity of the LEP appears to be close to that of the SLC. During the first year of operation, the accessible luminosities will probably be lower still. Different workers have therefore used values between 10^{30} and $10^{31} \text{ cm}^{-2}\text{s}^{-1}$ in their estimates.^{20,23}

The number N_h^θ of hadronic events associated with toponium decays and the number $N_h^{\gamma,Z}$ of background events due to the γ and Z^0 are, respectively, given by

$$N_h^\theta = \sigma_\mu R^\theta LT, \quad (63)$$

$$N_h^{\gamma,Z} = \sigma_\mu R^{\gamma,Z} LT, \quad (64)$$

where T is the time taken to acquire the statistics,

$$\sigma_\mu \equiv \sigma(e^+e^- \rightarrow \gamma^* \rightarrow \mu^+\mu^-) = \frac{4\pi\alpha^2}{3s} = \frac{86.8 \text{ nb}}{(W, \text{GeV})^2}, \quad (65)$$

$$R = \frac{\sigma(e^+e^- \rightarrow h)}{\sigma_\mu}, \quad (66)$$

and $W = s^{1/2}$ is the total center-of-mass energy.

Since calculations show that the total decay width of toponium (see Fig. 6) is appreciably smaller than the beam energy spread in accelerators, the peak width R and, hence, its height R_m^θ will be determined by the beam energy spread. For the SLC accelerator, this spread is planned to be quite large:

$$\Delta W|_{\text{SLC}} \approx \left(\frac{W, \text{GeV}}{10}\right)^2 \text{ MeV}, \quad (67)$$

and the figure for LEPI is lower by factor of about two.

The integrated area under the narrow resonance peak in R is given by

$$\int \Delta R(W) dW = \frac{9\pi}{2\alpha^2} \Gamma(\theta \rightarrow e^+e^-), \quad (68)$$

whence R_m^θ turns out to be

$$R_m^\theta = \frac{9\pi^{1/2}}{2\sqrt{2}\alpha^2} \frac{\Gamma_0(\theta) r_{e^+e^-} \text{Br}(\theta \rightarrow h)}{\Delta W}. \quad (69)$$

Radiative effects^{84,111} provide additional factors in (69) and, when all these are taken into account in the calculation,²³ the result for R^θ and $R^{\gamma,Z}$ is as shown in Fig. 15. These curves can now be readily used to determine the true experimental statistics from (63) and (64).

It is clear that, for toponium masses between 70 and 80 GeV, the signal-to-noise ratio is close to unity and varies appreciably (it falls from about 1.5 to about 0.5 as the mass increases). Nevertheless, the total number of events turns out to be appreciable even under such unfavorable conditions. According to Ref. 23, for luminosity $L = 1.1 \times 10^{31} \text{ cm}^{-2}\text{s}^{-1}$, $\Gamma_0 = 5 \text{ keV}$, and $\Delta W = 32 \text{ MeV}$, in one year of operation of the LEP, it is hoped to accumulate 14 000 cases involving the hadronic decay of toponium of mass 80 GeV against a background of 30 000 events. If the mass is 70 GeV, the background may even be somewhat lower than the signal level. We note that the background can be reduced by using additional selection criteria (see below).

Of course, under the conditions indicated above, the search for toponium will be very difficult and time-consuming in the absence of some information about its position, and such searches would occupy considerable amounts of time. It has therefore been suggested^{16,18,23} that the first step should be the determination of the threshold for the production of the bare top. This will be found either from the Z^0 decays or by measuring the aplanarity of events outside Z^0 . Actually, since the top quark is heavy, its decay products are emitted at large angles and do not lie in the same plane. An increase in the aplanarity of events beyond a certain threshold will therefore itself be an indication of the production of bare tops.

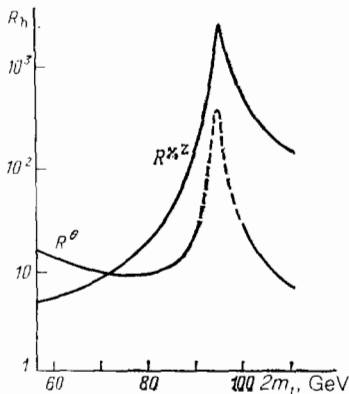


FIG. 15. The γ, Z (background) and θ (signal) contributions to R due to hadron production as functions of twice the mass of the top quark.²³ Interference effects may be important in the Z^0 region, so that R^θ is indicated by the broken curve.

Three methods have been proposed²³ for the determination of the mass of the top quark. The mass can be determined from the rate of production of the meson pair with the bare top in Z^0 decays (depending on their mass), from the energy spectra of leptons in semileptonic decays, and from multijet processes in nonleptonic weak decays of such mesons. The overall conclusion is that the mass of the top quark can be determined to within better than 500 MeV.

Estimates^{18,23} show that the range within which the toponium search should be made can thus be reduced to 2 GeV by scanning at intervals of $2\Delta W$ and recording the signal in the total hadron production cross section.

If we demand that, for each such interval, the signal must be within n standard deviations, the required integrated luminosity can be determined from the condition

$$LT\sigma_\theta = n^2 \left(1 + \frac{\sigma_B}{\sigma_\theta} \right), \quad (70)$$

where $\sigma_{B(\theta)}$ is the cross section for the background (toponium).

The ratio σ_B/σ_θ could be reduced by employing different selection criteria. For example, it has been suggested that it would be relatively simple to use "trust"^{113,114} T and "oblateness"¹¹⁵ O to separate noise from the signal if the individual quark decays play an important role, i.e., if the toponium mass is large (as can be seen from Fig. 6). The efficacy of this method is determined by the sharp difference between T and O distributions of background and toponium events (background cases lie practically on a single line on the T, O plane). This should enable us to separate out 95% of the background events and retain 87% of the signal (for a particular selection criterion).

The precision with which the mass of the 1S- and 2S-states can be measured is largely determined by systematic errors due to the beam energy spread. However, it does not influence the mass difference between these states. The precision with which this difference can be found²³ is of the order of 10–30 MeV. The leptonic width can be determined with a precision of up to 10–20%.

Searches for the higher radial excitations will be much more complicated because of the reduction in the leptonic width and level separations as the radial quantum number increases. However, potential models can predict their positions quite well and thus reduce the range of scanning. It has been suggested²³ that even the 7S-states may become amenable to this approach.

As already discussed, the most important basis (after the 2S- and 1S-levels) for verifying potential models and determining the potential itself is provided by determinations of the position of 1P-states. Radiative transitions between the 2S- and 1P-states are very noticeable in the potential with a step, whereas, for other potentials, they are significant only for low toponium masses (below 80 GeV). However, even in the latter case, there are arguments²³ in favor of the practical possibility of detection of such transitions with the LEP.

Different methods of detection have been proposed, including inclusive production of two photons in the $\theta' \rightarrow \gamma_1 \chi_1 \rightarrow \gamma_1 \gamma_2 \theta$ reaction, or the exclusive channel with the

decay of the θ into a leptonic pair $\theta' \rightarrow \gamma_1 \chi_t \rightarrow \gamma_1 \gamma_2 \theta \rightarrow \gamma_1 \gamma_2 l^+ l^-$. Even for a small separation (about 100 MeV) between the θ' and χ_t , Monte Carlo calculations²³ suggest that well-defined signals due to both photons should be seen. (Moreover, the first method is effective in this case for masses up to about 80 GeV, and the second may help in extending the range up to about 85–90 GeV.) For a potential with a step, the conditions for the observation of P-states are very much better.

An interesting (though exotic) possibility⁶² is the direct production of P-states in e^+e^- annihilation. Owing to the axial vector coupling, the Z^0 -boson can undergo a direct transition to the n^3P_1 -state ($J^{PC} = 1^{++}$). If the mass of the P-state of the χ_t is roughly equal to the mass of the Z^0 -boson, the χ_t will be created relatively frequently, and will produce a few tens of events per day. For masses outside the region of the Z^0 resonance, the χ_t production will, of course, be less noticeable.

There is, finally, another exotic possibility that must be borne in mind. Let us suppose that nature has provided us a fourth generation of quarks, and that its lightest member with charge 1/3 is lighter even than the top quark, or has a very similar mass. Analysis of this situation is substantially more complicated, and one can only hope that it may be possible to exploit the fact that the production cross section will be lower by a factor of four in this case than for the top quark, since it is proportional to the square of the charge.

8. CONCLUSIONS

The top quark remains the only quark in the standard model with three generations for which we have virtually no direct information. Nevertheless, there is a general hope (apparently, resting mainly on the preliminary results reported by the UA1 group²¹) that this quark will be discovered on the SLC and LEP accelerators, i.e., its mass will lie in the range between 30 and 50 GeV. If this hope is realized, it will also be possible to investigate the properties of the bound states of the top quark and its antiquark, i.e., toponium.

The small size of this system will enable us to investigate the interaction between current quarks and to examine the competition between strong and electroweak interactions. It will also provide us with the possibility of studying new particles.

In spectroscopic studies of the toponium family, basic information on the interaction between the quarks and toponium will be deduced even from the positions of the lowest lying 1S-, 2S-, and 1P-states and their leptonic widths.²⁵¹ The most interesting problem that will then have to be examined will be the *transition of current quarks to constituent quarks, and the property of asymptotic freedom* (the constant Λ_{QCD}).

Higher radial excitations will tell us *whether the quark interaction potential is flavor-independent*.

Although there may be about 10 such states, and the orbital angular momenta of the toponium system may even exceed 15, leading to a total number of levels of about 400, this abundance of possibilities will hardly be fully exploited,

mostly because the energy spread of the particles in the colliding beams will be large (tens or even hundreds of MeV), so that the problem of separating closely-spaced levels will become a difficult practical task.

The situation is complicated still further by the fact that the fine and hyperfine level splitting turns out to be no more than 10 MeV. It therefore seems to us that *relativistic effects* should be smaller than for bottomium and, moreover, the deterioration in the beam energy spread will make these effects difficult to observe.

The crucial point for the observation of toponium and for studying its decay properties is its actual mass. Masses of 80–85 GeV correspond to optimal properties of toponium from the point of view of traditional approach to quarkonia. If the mass differs from that of the Z^0 -boson by not more than 10–15 GeV, other electroweak effects such as interference between toponium and the Z^0 come into play, and the physics of toponium and of the Z^0 -boson becomes a single subject of investigation. Even if the mass of toponium is appreciably greater than that of the Z^0 , the situation will be dominated as the top-quark decays, i.e., typically electroweak processes. The conditions for observing toponium deteriorate appreciably with increasing mass, especially in the case of its radial excitations and states with nonzero orbital angular momentum.

As far as the decays of toponium are concerned, these decays are interesting mainly as a possible source of new particles (*scalar Higgs particles, superparticles, and ...?*) They can be regarded as a kind of laboratory for studying the situation with comparable *strong and electroweak interactions*.

New particles should be relatively readily observed if they are accessible kinematically and influence appreciably the fraction of different decays. The observation of semileptonic decays of the top quark by the UA1 group (if their interpretation is correct!) has therefore reduced hopes for new particles, to some extent.

Electroweak interactions begin to dominate heavy systems, and, with increasing mass of the ground state (and, even more so, all other states), the principal process is simply the decay of one of the quarks, which should provide us with a reliable means of measuring the *electroweak coupling of the top quark* (with an independent measurement of its *charge and isospin*) and of determining its *lifetime*.

Nevertheless, still in the region of the Z^0 , there is the important and interesting channel of decay into a neutrino and antineutrino, which may help us with the resolution of the problem of the *number of types of neutrino in nature*.

There seems to be a sufficiently firm prospect of the practical production and investigation of toponium on the SLC and LEP1 machines²³ throughout the energy range. This optimism is moderated, to some degree, by minor factors, since toponium will probably be the last of the quarkonia to be studied, even if there are still heavier quarks, and their electroweak decays will be so strong that they will not be able to form bound states, provided, of course, this region of short distances does not conceal some new and unexpected phenomena.

I am indebted to E. L. Feinberg, M. A. Shifman, and V. A. Khoze for valuable suggestions.

APPENDIX

Theoretical calculations of decay probabilities, the results of which are given in Sec. 6, are, unfortunately, subject to a number of uncertainties. Formulas (29)–(37), which give the probability ratios for toponium decays, are based on a simple tree approximation. On the other hand, there are calculations of the quantum chromodynamic radiative corrections to annihilation decays, which we shall now discuss. Because the coupling constant α_s is large, these corrections are not always sufficiently small to enable us to conclude that the series converges. They sometimes reach 20% or even 50%. The other problem relates to the choice of scale for the calculation of the coupling constants.

Unfortunately, the QCD corrections are unknown for one of the most important decays, namely, the decay of the single quark.

In the case of the decay of toponium into a Higgs particle and a photon, the corrections to (29) are¹¹⁹

$$r_{H^0\gamma} = r_{H^0\gamma}^0 \left[1 - \frac{4}{3} \frac{\alpha_s}{\pi} f(z) \right], \quad (\text{A.1})$$

where $r_{H^0\gamma}^0$ is given by (29),

$$f(z) = -\frac{\pi^2}{12(1-z)} - \frac{F(1-2z)}{2(1-z)} + \frac{z-1}{1-2z} + \frac{2z(z-2)}{(1-z)^2} \\ \times [\Phi(z) + F(1) - F(-1)] \\ + \left[4 + \frac{4}{z} + \frac{8}{1-z} \right] \left(\frac{z}{1-z} \right)^{1/2} \text{arctg} \left(\frac{z}{1-z} \right)^{1/2} \\ + \left[2 + \frac{4}{1-z} + \frac{z}{(1-2z)^2} \right] \ln 2 + \ln(1-z),$$

$$z = \frac{m_{H^0}^2}{m_t^2}, \quad F(x) = \int_0^x \frac{dy}{y} \ln(1+y),$$

$$\Phi(x) = \int_0^1 \frac{dy}{y-(x/2)} \ln \frac{1-4y(1-y)x}{2y(1-x)},$$

and the scale of α_s can only be determined from second-order corrections.

It is readily seen that the above corrections are very large if the mass of the Higgs particle is close to that of toponium ($z \rightarrow 1$), and predictions become very uncertain in this region.

In the case of decay into three gluons, the corrections to (30) are as follows:^{120,121}

$$r_{ggg} = r_{ggg}^0 \left[1 + \frac{\alpha_{\overline{\text{MS}}}(m_t)}{\pi} (2.77b_0 - 14) \right], \quad (\text{A.2})$$

whereas, in the decay into two gluons and a photon [see (31)]

$$r_{gg\gamma} = r_{gg\gamma}^0 \left[1 + \frac{\alpha_{\overline{\text{MS}}}(m_t)}{\pi} \left(2.77 \frac{2}{3} b_0 - 11.8 \right) \right], \quad (\text{A.3})$$

where

$$b_0 = \frac{1}{3} (33 - 2n_f),$$

$$b_1 = \frac{1}{3} (306 - 22n_f),$$

$$\alpha_{\overline{\text{MS}}}(q^2) = \frac{4\pi}{b_0 \ln(q^2/\Lambda_{\overline{\text{MS}}}^2)} - \frac{4\pi b_1}{b_0^2} \frac{\ln \ln(q^2/\Lambda_{\overline{\text{MS}}}^2)}{\ln^2(q^2/\Lambda_{\overline{\text{MS}}}^2)},$$

for $n_f = 5$, $2.77b_0 - 14 \approx 7.2$, $2.77 \cdot (2/3)b_0 - 11.8 \approx 2.4$.

We note that the radiative corrections to the decay width and the correction term in the leptonic width (27) have opposite signs, i.e., the effect of the QCD corrections increases sharply when we analyze the corresponding width ratios.

Let us also consider the correction terms for the hyperfine splitting ΔE_{ss}^0 (26), calculated in Refs. 122 and 123:

$$\Delta E_{ss} = \Delta E_{ss}^0 \left\{ 1 + \frac{\alpha_{\overline{\text{MS}}}(m_t)}{\pi} \left[-\frac{8}{3} - \frac{3}{4} \ln 2 \right. \right. \\ \left. \left. + \frac{21}{8} \xi + \frac{1}{4} b_0 \left(\frac{5}{3} - \xi \right) \right] \right\}, \\ \xi = \left\langle \ln_t \frac{q^2}{m_t^2} \right\rangle |\Psi(0)|^{-2}, \quad (\text{A.4})$$

where the averages are evaluated with the toponium wave functions.

As far as the parameter $\Lambda_{\overline{\text{MS}}}$ in (A.1)–(A.4) is concerned, it is well-known⁶⁷ that the information on this quantity deduced from different experiments turns out to be somewhat different, although, for practical estimates, it is probably safe to assume that $\Lambda_{\overline{\text{MS}}}$ is about 150–200 MeV.

¹¹⁹All three families of particles with hidden flavor that consist of a heavy quark and its antiquark ($c\bar{c}$, $b\bar{b}$, and $t\bar{t}$) are given the common name of *quarkonia*.

¹²⁰The precision with which the masses are measured is so high that the errors affect only the last figure.

¹²¹We are using the spectroscopic notation for quarkonia, described above.

¹²²Here and henceforth, we use the system of units with $\hbar = 1$, $c = 1$, i.e., the relativistic notation, since this does not give rise to any complications.

¹²³The experimental information on quarkonia corresponds to this case, as we saw in the last Section.

⁶⁷We note that asymptotic freedom (for $\epsilon = -1$) leads to a radial dependence of κ of the form $\ln^{-1}r$, which makes the potential shallower thus causing the Coulomb dependences to become closer (although not very much) to the case of charmonium and bottomium. The change in the qualitative dependence of different variables as we pass to toponium can be appreciated in a crude way by comparing their dependence on the mass of the system for $\epsilon \ll 1$ (charmonium, bottomium) and $\epsilon \approx -1$. In the two cases that we are examining, the conditions of theory (3) discussed above are satisfied and, therefore, the 1P-state lies below the 2S-state.

⁷This problem is closely related to the Klein paradox and is explained by the instability of the "Dirac sea" in strong fields.

⁸The arguments in favor of this choice of potential can also be based¹¹⁷ on the sum rule for heavy quarkonia, written out, for example, in Ref. 116. The predicted^{53,54} toponium spectrum easily satisfies the sum rules, whereas other choices lead to large differences.

⁹Following Ref. 23, we shall represent the toponium levels by $\theta, \theta', \dots, \chi_1, \dots$.

¹⁰Its order of magnitude is usually about 0.1% of the beam energy.

¹¹For the moment, we confine our attention to the nonrelativistic problem without fine and hyper-fine splitting (which will be discussed later).

¹²This result is not surprising if we recall that, in the potential well, not only the 1P- but even the 1D-level lie below the 2S-level. The step which acts as an additional potential well forces the 1P level downward.

¹³This corresponds to a "jump" in the charge, i.e., an abrupt change in the Lorentz-vector part of the potential, which seems less probable than the

change in the Lorentz-scalar component, discussed above.

- ¹⁴The relative position of the levels can be determined from the photon energies in radiative transitions.
- ¹⁵The tensor splitting is usually small.
- ¹⁶In particular, the constant difference between the squares of the masses of the 3S_1 - and 1S_0 -levels, predicted for quarkonia, will no longer be valid here. However, the corresponding verification is complicated by the fact that the splitting is small.
- ¹⁷W-boson exchange corresponds to such short distances that the wave function of toponium can also be taken at a single point. Generally, all effects due to very short-range forces are considered to be proportional to $|R(0)|^2$; see, for example, (26). Hence, using (27), we have $\Delta E_{\text{ss}}/\Gamma_0 \approx 2\alpha_s/\alpha^2$, which is in reasonable agreement even in the case of charmonium, when radiative corrections are taken into account [see also the remarks relating to (26)].
- ¹⁸The UA1 results² obtained on the Sp \bar{p} S collider for electrons from top-quark decays exclude charged Higgs scalars with mass $m(H^\pm) < m_t - 5 \text{ GeV}$ (if we adopt the interpretation based on the assumed creation of toponium).
- ¹⁹Appreciable mixing angles for different generations would be an indication of the preon structure of quarks.¹¹⁸
- ²⁰However, it may be important for counting the number of types of neutrino (see Sec. 6.5).
- ²¹The formula given by (40) includes summation over all the 3P_J -levels, since, as already discussed above, fine splitting is very small and it is difficult to separate the individual levels.
- ²²According to Ref. 23, the mass can actually be measured to within better than 1 GeV.
- ²³We note, however, that the radiative corrections to (29) are large, and this throws doubt on its validity (see Appendix).
- ²⁴If we ignore depolarization due to the hadronization of the quark.
- ²⁵According to the estimates given in Ref. 23, if the mass of toponium is less than that of the Z^0 -boson (about 70 GeV), the detection and investigation of the 1S- and 2S-states will need less than two months of LEP time. For the 1P- and 3S-5S-states, the corresponding times are six months and up to eight months, respectively.

¹M. Althoff *et al.*, Phys. Lett. B **147**, 441 (1984).

²G. Arnison *et al.*, *ibid.* 493.

³A. I. Vainshtein *et al.*, Usp. Fiz. Nauk **123**, 217 (1977) [Sov. Phys. Usp. **20**, 796 (1977)].

⁴B. Richter, Rev. Mod. Phys. **49**, 251 (1977) [Russ. transl., Usp. Fiz. Nauk **125**, 201 (1978)].

⁵S. C. C. Ting, Rev. Mod. Phys. **49**, 235 (1977) [Russ. transl., Usp. Fiz. Nauk **125**, 227 (1978)].

⁶T. Appelquist, N. M. Barnet, and K. D. Lane, Ann. Rev. Nucl. Part. Sci. **28**, 387 (1978).

⁷C. Quigg and J. L. Rosner, Phys. Rep. **56**, 167 (1979).

⁸M. Krammer and H. Krasemann, Acta. Phys. Aust. Suppl. **21**, 259.

⁹A. I. Vainshtein *et al.*, Usp. Fiz. Nauk **131**, 537 (1980) [Sov. Phys. Usp. **23**, 429 (1980)].

¹⁰E. Reya, Phys. Rep. **69**, 195 (1981).

¹¹M. Bander, *ibid.* **75**, 205.

¹²A. Martin, Preprints CERN Ref. TH3162-1981; TH3397-1982; TH4161/85-1985; TH4382/86-1986.

¹³E. D. Bloom, Preprint SLAC-PUB-3015, 1982.

¹⁴V. A. Khoze and M. A. Shifman, Usp. Fiz. Nauk **140**, 3 (1983) [Sov. Phys. Usp. **26**, 387 (1983)].

¹⁵M. E. Peskin, Preprint SLAC-PUB-3273-1983.

¹⁶E. D. Bloom and G. J. Feldman, Sci. Am. **246**(5), 66 (May 1982) [Russ. transl., Usp. Fiz. Nauk **139**, 529 (1983)].

¹⁷A. A. Bykov, I. M. Dremin, and A. V. Leonidov, Usp. Fiz. Nauk **143**, 3 (1984) [Sov. Phys. Usp. **27**, 321 (1984)].

¹⁸T. Himel, Preprint SLAC-PUB-3510, 1984.

¹⁹J. H. Kühn, Preprint CERN-TN-4083/84, 1984.

²⁰E. Eichten, Preprint Fermilab-Conf.-85/29-T, 1985.

²¹C. Quigg, Preprint Fermilab-Conf.-85/126-T, 1985.

²²S. Cooper, Preprint SLAC-PUB-3819, 1985.

²³W. Buchmüller *et al.*, Preprint MPI-PAE/PTH 85/85, 1985.

²⁴M. E. B. Franklin, Preprint SLAC-254, 1982.

²⁵J. E. Gaiser, Preprint SLAC-255, 1982.

²⁶K. F. Einsweiler, Preprint SLAC-272, 1984.

²⁷R. A. Lee, Preprint SLAC-282, 1985.

²⁸G. Alexander and A. Fridman, Riv. Nuovo Cimento **4**, 1 (1981).

²⁹K. Berkelman, Phys. Rep. **98**, 145 (1983).

³⁰R. Nernst *et al.*, Preprints SLAC-PUB-3571, -3820, 1985.

³¹D. M. Gelfman, Preprint SLAC-286, 1985.

³²J. L. Richardson, Phys. Lett. B **82**, 272 (1979).

³³W. Buchmüller, G. Grunberg, and S. H. H. Tye, Phys. Rev. Lett. **45**, 103 (1980).

³⁴W. Buchmüller and S. H. H. Tye, Phys. Rev. D **24**, 132 (1981).

³⁵A. Martin, Preprints CERN TH-4060/84, 1984; 6604/85, 1985.

³⁶B. Baumgartner, H. Crosse, and A. Martin, Phys. Lett. B **146**, 363 (1984).

³⁷A. Martin, *ibid.* **100**, 4511 (1981).

³⁸H. D. Politzer, Nucl. Phys. B **117**, 397 (1976).

³⁹I. V. Andreev, Yad. Fiz. **41**, 1345 (1985) [Sov. J. Nucl. Phys. **41**, 855 (1985)].

⁴⁰M. S. Plesset, Phys. Rev. **41**, 278 (1932).

⁴¹M. E. Rose, *ibid.* **82**, 470 (1951).

⁴²H. J. Schnitzer, Phys. Rev. D **18**, 3482 (1978).

⁴³G. Fogleman *et al.*, Nuovo Cimento Lett. **26**, 369 (1979).

⁴⁴E. Eichten and G. Feinberg, Phys. Rev. D **23**, 2724 (1981).

⁴⁵D. B. Lichtenberg *et al.*, Phys. Lett. B **113**, 267 (1982).

⁴⁶W. Buchmüller, *ibid.* **112**, 479.

⁴⁷G. Hardekopf and J. Sucher, Phys. Rev. D **25**, 2939 (1982).

⁴⁸H. Grotch and K. J. Sebastian, *ibid.* 2944.

⁴⁹C. Long and D. Robson, *ibid.* **27**, 644 (1983).

⁵⁰A. D. Steiger, Phys. Lett. B **129**, 335 (1983).

⁵¹M. Frank and P. J. O'Donnell, *ibid.* **159**, 174 (1985).

⁵²I. M. Dremin and A. V. Leonidov, Pis'ma Zh. Eksp. Teor. Fiz. **37**, 617 (1983) [JETP Lett. **37**, 738 (1983)].

⁵³A. A. Bykov and I. M. Dremin, *ibid.* **42**, 119 (1985) [JETP Lett. **42**, 146 (1985)].

⁵⁴A. A. Bykov and I. M. Dremin, Yad. Fiz. **44**, 652 (1986) [*sic*].

⁵⁵M. B. Voloshin, Nucl. Phys. B **154**, 365 (1979).

⁵⁶H. Leutwyler, Phys. Lett. B **98**, 447 (1981).

⁵⁷A. A. Ansel'm, N. G. Ural'tsev, and V. A. Khoze, Usp. Fiz. Nauk **145**, 185 (1985) [Sov. Phys. Usp. **28**, 113 (1985)].

⁵⁸C. Quigg and J. L. Rosner, Phys. Lett. B **72**, 462 (1978).

⁵⁹E. Eichten and K. Gottfried, *ibid.* **66**, 286 (1977).

⁶⁰H. Krasemann and S. Ono, Nucl. Phys. B **154**, 283 (1979).

⁶¹A. A. Bykov, I. M. Dremin, and A. V. Leonidov, Yad. Fiz. **39**, 977 (1984) [Sov. J. Nucl. Phys. **39**, 618 (1984)].

⁶²J. H. Kühn and S. Ono, Z. Phys. C **21**, 395 (1984); **24**, 404(E).

⁶³S. Güsken, J. H. Kühn, and P. M. Zerwas, Nucl. Phys. B **262**, 393 (1985).

⁶⁴V. Abe *et al.*, Phys. Rev. D **27**, 675 (1983).

⁶⁵W. Fischer, Nucl. Phys. B **129**, 157 (1977).

⁶⁶W. Celmaster *et al.*, Phys. Rev. D **17**, 879 (1978).

⁶⁷D. W. Duke and R. G. Roberts, Phys. Rep. **120**, 275 (1985).

⁶⁸W. Buchmüller, Y. J. Ng, and S. H. Tye, Phys. Rev. D **24**, 3003 (1981).

⁶⁹M. A. Shifman *et al.*, Nucl. Phys. B **147**, 385, 448 (1979).

⁷⁰M. B. Voloshin, *ibid.* **154**, 365.

⁷¹M. B. Voloshin, Preprints ITEP-21, Moscow, 1980; ITEP-30, Moscow, 1981.

⁷²C. Callan *et al.*, Phys. Rev. D **18**, 4684 (1978).

⁷³E. V. Shurvak, Phys. Rep. **115**, 151 (1984).

⁷⁴V. N. Baier and Yu. F. Pinelis, Preprint INP 82-115, Novosibirsk, 1982; 83-62, Novosibirsk, 1983.

⁷⁵H. Leutwyler, Phys. Lett. B **98**, 447 (1981).

⁷⁶J. Ellis and M. K. Gaillard, Preprints CERN 76-18, Geneva, 1976; 79-01, Geneva, 1979.

⁷⁷J. Kühn, Acta Phys. Pol. B **12**, 347 (1981).

⁷⁸L. M. Sehgal and P. M. Zerwas, Nucl. Phys. B **183**, 417 (1981).

⁷⁹V. A. Matveev, B. V. Struminskiĭ, and A. N. Tavkhelidze, Preprint OIYaI R2524, Moscow, 1965.

⁸⁰V. Van Royen and W. Weisskopf, Nuovo Cimento **50**, 617 (1967).

⁸¹F. Wilczek, Phys. Rev. Lett. **39**, 1304 (1977).

⁸²I. I. Bigi and H. Krasemann, Z. Phys. C **7**, 127 (1981).

⁸³J. Kühn and K. H. Streng, Nucl. Phys. B **198**, 71 (1982).

⁸⁴L. N. Lipatov and V. A. Khoze, Trudy XI Shkoly LiYaF (Proc. Eleventh School of the Leningrad Institute of Nuclear Physics), Leningrad, 1975.

⁸⁵Y. P. Kuang and T. Yan, Phys. Rev. D **24**, 2874 (1981).

⁸⁶T. M. Yan, *ibid.* **22**, 1652 (1980).

⁸⁷M. I. Vysotskiĭ, Usp. Fiz. Nauk **146**, 591 (1985) [Sov. Phys. Usp. **28**, 667 (1985)].

⁸⁸H. P. Nilles, Phys. Rep. **100**, 1 (1984).

⁸⁹H. E. Haber and G. L. Kane, *ibid.* **117**, 75 (1985).

⁹⁰B. A. Campbell, J. Ellis, and S. Rudaz, Nucl. Phys. B **198**, 1 (1982).

⁹¹E. Reya and P. P. Roy, Phys. Lett. B **141**, 442 (1984); Phys. Rev. Lett. **53**, 881 (1984).

- ⁹²J. Ellis and H. Kowalski, Nucl. Phys. B **246**, 199 (1984); Phys. Lett. B **142**, 441 (1984).
- ⁹³J. Ellis and S. Rudar, *ibid.* **128**, 248 (1983).
- ⁹⁴B. A. Campbell, J. A. Scott, and M. K. Sundaresan, *ibid.* **131**, 213.
- ⁹⁵J. H. Kuhn, Phys. Lett. B **141**, 433 (1984).
- ⁹⁶W. Y. Keung, Phys. Rev. D **28**, 1129 (1983); **29**, 1544(E) (1984).
- ⁹⁷S. Samuel and J. Wess, Nucl. Phys. B **221**, 153 (1983).
- ⁹⁸O. Nachtmann, A. Reiter, and M. Wirbel, Z. Phys. C **23**, 85 (1984).
- ⁹⁹I. Y. Bigi, J. H. Kuhn, and H. Schneider, Preprint MPI-PAE/PTh 28, 1978.
- ¹⁰⁰J. Bernabeu and P. Pascual, Phys. Lett. B **87**, 69 (1979); Nucl. Phys. B **172**, 93 (1980).
- ¹⁰¹R. Koniuk, R. Leroux, and N. Isgur, Phys. Rev. D **117**, 2915 (1978).
- ¹⁰²R. Budny, *ibid.* **20**, 2763 (1979).
- ¹⁰³B. Grzadkowski *et al.*, Preprint CERN-TH-4226, Geneva, 1985.
- ¹⁰⁴I. Y. Bigi and H. Krasemann, Z. Phys. C **7**, 127 (1981).
- ¹⁰⁵J. H. Kühn and F. Wagner, Nucl. Phys. B **236**, 16 (1984).
- ¹⁰⁶F. M. Renard, Z. Phys. C **1**, 225 (1979).
- ¹⁰⁷P. J. Franzini and F. J. Gilman, Phys. Rev. D **32**, 237 (1985).
- ¹⁰⁸J. H. Kühn and P. M. Zerwas, Phys. Lett. B **154**, 448 (1985).
- ¹⁰⁹L. J. Hall, S. F. King, and S. R. Sharpe, Nucl. Phys. B **260**, 510 (1985).
- ¹¹⁰A. Martin, Phys. Lett. B **156**, 411 (1985).
- ¹¹¹J. D. Jackson and D. L. Scharre, Nucl. Instrum. Methods **128**, 13 (1975).
- ¹¹²G. Goggi and G. Penso, Nucl. Phys. B **165**, 429 (1960).
- ¹¹³S. Brandt *et al.*, Phys. Lett. **12**, 57 (1964).
- ¹¹⁴E. Farhi, Phys. Rev. Lett. **39**, 1587 (1977).
- ¹¹⁵D. Barber *et al.*, *ibid.* **43**, 830 (1979).
- ¹¹⁶A. Nicolaidis and G. J. Gounaris, Phys. Rev. D **30**, 996 (1984).
- ¹¹⁷A. A. Bykov, *Kratk. Soobshch. Fiz.* No. 12, 41 (1986) [Sov. Phys. Lebedev Inst. Rep. No. 12, in press (1986)].
- ¹¹⁸F. N. Renard, Preprint SLAC-PUB-3028, 1982.
- ¹¹⁹M. I. Vysotsky, Phys. Lett. B **97**, 159 (1980).
- ¹²⁰P. B. Mackenzie and G. P. Lepage, Phys. Rev. Lett. **47**, 1244 (1981).
- ¹²¹S. J. Brodsky, G. P. Lepage, and P. B. Mackenzie, Phys. Rev. D **28**, 228 (1983).
- ¹²²R. Barbieri, R. Gatto, and E. Remiddi, Phys. Lett. B **106**, 497 (1981).
- ¹²³S. N. Gupta, S. F. Radford, and W. W. Repko, Phys. Rev. D **26**, 3305 (1982).

Translated by S. Chomet